

THERMODYNAMICS OF CeNiSn AT LOW TEMPERATURES AND IN WEAK MAGNETIC FIELDS

K.A. Kikoin¹, M.N. Kiselev^{2,3}, A.S. Mishchenko², and A. de Visser⁴

¹ *Ben-Gurion University of the Negev, Beer-Sheva 84105, Israel*

² *Russian Research Center "Kurchatov Institute", Moscow 123182, Russia*

³ *Laboratoire Leon Brillouin, CE-Saclay 91191 Gif-sur-Yvette Cedex, France*

⁴ *Van der Waals-Zeeman Institute, University of Amsterdam,
Valckenierstraat 65, 1018 XE Amsterdam, The Netherlands*

(August 2, 2018)

Detailed experimental and theoretical studies of the low-temperature specific heat, magnetic susceptibility, thermal expansion and magnetostriction of the orthorhombic compound CeNiSn are presented. All anomalies observed in the thermodynamic and magnetic properties of CeNiSn are explained in a framework of a model of metallic Kondo lattice with well developed spin-liquid-type excitations. The pseudogap behavior of these excitations appears due to interplay between spin-fermions and soft crystal-field (CF) states. The thermodynamic relations for the spin liquid are derived. Together with the explanation of inelastic neutron scattering spectra given earlier within a same approach these studies of the low-temperature thermodynamics and magnetic response give a consistent description of the nature of anomalies in the low-temperature thermodynamics of perfect and imperfect CeNiSn crystals.

PACS numbers: 75.10.Dg, 75.30.Mb, 71.70.Gm

I. INTRODUCTION

The orthorhombic compounds CeNiSn and CeRhSb are known as Kondo lattice systems with peculiar thermodynamic and magnetic properties. Unusual features are observed at low temperatures $T < T^*$ in the specific heat, the thermal expansion coefficient, the magnetic susceptibility, the magnetostriction, and the NMR relaxation rate (see [1,2] for a review of early data). The characteristic temperature T^* is $\sim 10K$ for both systems. It should be emphasized that this temperature is much less than the Kondo temperature T_K estimated by standard methods, e.g., extracted from the logarithmic high-temperature dependence of the electrical resistivity. In the early measurements the electrical resistivity showed an upturn at low temperatures in the temperature region $T < T^*$. This upturn was interpreted as the indication to a non-metallic ground state of these systems, and the energy gap in the heavy electron spectrum was claimed to be responsible for the peculiar behavior of CeNiSn and CeRhSb. These materials together with the cubic Ce- and U-based compounds, Ce₃Sb₄Pt₃ or U₃Bi₄Pt₃ were classified as "Kondo insulators" [3].

Later on it turned out that significant differences exist between the real-gap cubic semiconductors and the orthorhombic CeNiSn family (see [4] for a review). Most striking was the observation that the CeNiSn single crystals of good quality show metallic character of the resistivity [5] at very low temperatures, and such behavior seems to be incompatible with the idea of a gap or pseudogap in the electron spectrum. Comparing the metallic behavior of electron transport with the anomalous low-temperature thermodynamics, one could suspect that the electronic spectrum with the pseudogap used in early phenomenological theories hardly can be responsible for all low- T peculiarities observed in the physical properties of CeNiSn and CeRhSb. Meaningful, e.g., is the fact that the unusual temperature dependence of the NMR relaxation rate $1/T_1 \sim T^3$ which was explained by the V-shape form of the density of electron states around the chemical potential at the bottom of the pseudogap [1] is observed exactly in the same temperature interval where the conventional Fermi-liquid-type T^2 law is seen for the electrical resistivity [5]. At $T < 1K$ the relaxation rate obeys the linear- T Korringa law characteristic for fermions with constant density of states [6]. One more striking feature of the low-energy excitations in CeNiSn is the extremely complicated (\mathbf{Q}, ω) -dependent structure of the inelastic magnetic scattering spectra that was observed in the same temperature region $T < T^*$ [7,8]. In gross features these unusual spectra also can be interpreted in terms of a pseudogap in the spin-excitation spectrum [9], although this phenomenology seems to be too simplistic to explain numerous details of the highly anisotropic neutron scattering cross section.

The theoretical approaches to the problem either implement the idea of a Kondo insulator with all its shortcomings, or try to offer alternative mechanisms which are based on a metallic type of electron spectra and seek the explanation of low-temperature thermodynamics and magnetic response in the unusual properties of the magnetic excitations. In the first case the starting point of the theory is the mean-field slave-boson approximation to the Anderson lattice [10,11]. The latest version of mean-field hybridization theory [9] refers to the actual symmetry of f-electron states

in the orthorhombic crystal. Since this procedure implies strong coupling of spin and charge degrees of freedom, the gap (or pseudogap) in the excitation spectrum necessarily means a semiconductor or semimetallic type of electrical resistivity which, apparently, contradicts the experimental data mentioned above.

An alternative approach was offered in Ref. [12]. In this theory new characteristic features with an energy scale of $T \ll T_K$ appear in the spectrum of the spin excitations due to the interplay between the non-local (spin-liquid) excitations characterized by the energy scale of T_K and the single-site crystal field (CF) excitations with the energy $\Delta_{CF} < T_K$. Within this model the semi-quantitative description of the low-energy specific heat and the thermal expansion coefficient was given in Ref. [13]. The CF levels are not seen directly neither in CeNiSn, nor in CeRhSb [1], and this result indicates that these local excitations are "dissolved" in the continuum of low-energy excitations of the Kondo lattice. However, the indirect estimate of the magnitude of crystal field created by the Ni ions on the Ce site [14] confirmed the validity of the inequality $\Delta_{CF} < T_K$.

Basing on the available experimental data related to the structure of magnetic excitations in CeNiSn, the quantitative theory of interplay between heavy fermions and CF excitations in CeNiSn was offered in Ref. [15]. The theory involves the idea of spin-liquid excitations of resonating valence bond (RVB) type which transform at low temperature into well defined fermions with their own dispersion predetermined by dispersion of RKKY exchange in the Brillouin zone [16]. As a result of the interplay between these excitations and soft CF states, the spectrum of spin-fermions in the low-symmetry lattice of CeNiSn transforms in such a way that the a deep minimum appears in the spin density of states (DOS) in the vicinity of the spinon Fermi level. Since the spin-liquid excitations are decoupled from the charged Fermi-liquid excitations in the conduction band, the gap in the spin DOS does not imply a corresponding gap in the electron DOS, and the system possesses metallic conductivity whereas the spin excitations are responsible for the thermal properties. It was shown in Ref. [15] that the inelastic transitions between the spinon states in the Brillouin zone are responsible for the complicated picture of inelastic magnetic neutron scattering. The successful attempt of the quantitative description of the magnetic scattering function $S(\mathbf{Q}, \hbar\omega)$, gives us strong arguments in favor of the existence of spin-liquid correlations in CeNiSn and related materials. Moreover, the fitting of the theoretical spectra to the experimental $S(\mathbf{Q}, \hbar\omega)$ provided us the values of the model parameters. With these data at hand we are able to give a quantitative description of the temperature dependence of various thermodynamical functions on the assumption [12,13] that the spin-liquid-type excitations give the main contribution to the low- T thermodynamics. Thus, a unified description of the low-temperature and low-energy properties of the orthorhombic CeNiSn family becomes possible.

The main purpose of the present paper is to give a detailed experimental and theoretical picture of the low-temperature specific heat, magnetic susceptibility, thermal expansion and magnetostriction coefficients in the CeNiSn family. This description should be consistent with the picture of magnetic excitations, as given by the inelastic neutron scattering experiments. Some of the experimental data for CeNiSn and CeRhSb were published in Refs. [13,17]. The first attempts of describing the inelastic magnetic spectra, low-temperature specific heat, and thermal expansion of these systems by using the same model [15,18] demonstrated the validity of the spin-liquid description.

II. EXPERIMENTAL

The magnetostriction of single-crystalline CeNiSn was measured in magnetic fields up to 8 T at selected temperatures of 0.5, 1.4 and 4.3 K. The magnetostriction is defined by $\lambda = (L(B) - L(0))/L(0)$, where $L(0)$ is the length of the specimen along a certain crystallographic direction in zero magnetic field. The magnetic field was always applied along the orthorhombic a -axis, while λ was measured along the field direction (λ_a) and perpendicular to the field direction along the b - (λ_b) and the c -axis (λ_c). The volume magnetostriction is defined by $\lambda_v = \lambda_a + \lambda_b + \lambda_c$ for a fixed field direction. The field was applied along the a -axis because this is the easy axis for magnetization: the low-temperature susceptibility χ_a is about a factor two larger than χ_b and χ_c , and, moreover χ_a exhibits a pronounced maximum at 12 K.

The experiments were carried out on a Czochralski grown single-crystalline sample. The sample was shaped by means of spark erosion into a cube with edges along the principal axes of the orthorhombic unit cell ($a \times b \times c \approx 2 \times 2 \times 2\text{mm}^3$). The magnetostriction was measured using a sensitive parallel-plate capacitance cell machined of oxygen free high-conductivity copper. The magnetostriction cell was fixed to the cold plate of a ^3He -insert, which is operated with an adsorption pump. The ^3He -insert could be placed in a superconducting solenoid with $B_{max} = 8$ T. The magnetostriction was measured by recording the capacitance, while slowly sweeping the field. Temperatures were stabilized by regulating on a field-insensitive RuO_2 chip-resistor which served as thermometer.

The experimental results are shown in Fig. 1a-c, while the coefficients of magnetostriction $\lambda'_i = L^{-1}dL/dB$, obtained by differentiating the data of Fig. 1 with respect to the field, are shown in Fig. 2a-c. At the highest temperature, $T = 4.3$ K, λ_i ($i = a, b, c$) is a monotonous function of the field. The crystal expands in $a - b$ plane and shrinks along

c -axis when $B \parallel a$. The magnetostriction is anomalous in the sense that the curves $\lambda'_i(B)$ deviate from the standard linear behaviour for paramagnetic systems. At lower temperatures this anomalous behaviour becomes stronger and dL_i/dB change their signs with increasing field. For instance, at $T = 0.5$ K, the $a - b$ plane shrinks till ~ 4.5 T and the c -axis expands till ~ 7 T. The anomalous behavior is also seen in the volume magnetostriction as a negative contribution at low temperatures, although is not very pronounced.

The magnetostriction data are in good agreement with previous thermal expansion measurements in zero and applied magnetic fields ($B \parallel a$) of 4 and 8 T, taken on the same single-crystalline specimen [13]. Strong anisotropy is observed in the linear expansion ($\alpha_i = L^{-1}(dL_i/dT)$): the dependence $\alpha_c(T)$ is anomalous with respect to $\alpha_{a,b}(T)$. In magnetic field a sign reversal takes place at low temperatures ($T < 3$ K at 8 T): $\alpha_c(T)$ becomes negative, while α_a and α_b become positive. The $\alpha_i(T)$ -curves show several anomalies, but the coefficient of volume expansion, $\alpha_v = \alpha_a + \alpha_b + \alpha_c$, is monotonous. Our magnetostriction data are also in excellent agreement with the data reported in Ref. [19] in the temperature range 0.1- 4.2 K and field range up to 20 T.

It is known that the reversible volume magnetostriction is thermodynamically equivalent to the strain dependence of the magnetic susceptibility $\chi(B, T)$ [20]

$$\lambda'_V(B, T) = \kappa_T B \left(\frac{\partial \chi(B, T)}{\partial \log V} \right)_{T, B} \quad (1)$$

(the magnetic susceptibility is defined as $\chi(B, T) = M(B, T)/B$, where $M(B, T)$ is the magnetization). Therefore, one can extract from the experimental result the field and temperature dependence of the magnetic susceptibility volume derivative $(\partial \chi(B, T)/\partial \log V)_{B, T}$. Introducing the doubly differential magnetostriction coefficient

$$\lambda''_V(B, T) = B^{-1}(d\lambda_V/dB)_{V, T} \quad (2)$$

one can express the logarithmic volume derivative of the magnetic susceptibility as

$$\left(\frac{\partial \chi(B, T)}{\partial \log V} \right)_{V, T} = \frac{\lambda''_V(B, T)}{\kappa_T} \quad (3)$$

It is seen from Fig. 3 that the temperature and field dependence of the volume derivative of the magnetic susceptibility deviates from the normal temperature and field independent behaviour at low temperatures and in low magnetic fields.

III. HAMILTONIAN AND THE ENERGY OF THE SPIN LIQUID

The orthorhombic compounds CeNiSn and CeRhSb are usually classified as Kondo lattices with moderately heavy fermion (HF) properties. The basic Hamiltonian which describes the Ce-based HF systems is the Anderson lattice Hamiltonian for the $\text{Ce}^{3+}(f^1)$ ion hybridized with the conduction electrons. In the Kondo lattice limit when the valence of the Ce ion is close to integer, one deals with well localized f -electrons for which the inequality $V_{kF\Lambda}^i \ll \epsilon_F - E_\Gamma$ is believed to be valid (here $V_{k\Lambda}^i$ is the hybridization matrix element between the f -electron localized on a site \mathbf{i} in a state $|\Lambda\rangle = |\Gamma\nu\rangle$ with the energy E_Γ of the f -electron in a crystal field and the partial component of the Bloch wave $|k\Lambda\rangle$, ν is the row of the irreducible representation Γ of the crystal point group, ϵ_F is the Fermi energy of conduction electrons). This hybridization integral is taken in the Coqblin-Cornut (CC) approximation [22] which represents the Bloch functions by their partial waves $c_{k\Lambda}^\dagger$, and takes into account only the diagonal in Λ hybridization matrix elements $V_{k\Lambda}^i = \langle k\Lambda|V|\mathbf{i}\Lambda\rangle$. Then the hybridization effects are reduced to exchange-like interaction between the localized f -electrons and the conduction electrons with an effective coupling constant

$$J_{\mathbf{i}}^{\Lambda\Lambda'}(k, k') = V_{k\Lambda}^{\mathbf{i}*} V_{k'\Lambda'}^{\mathbf{i}} / (\epsilon_k - E_\Gamma).$$

As was shown in [12,15], the non-CC hybridization $\bar{V}_{k\Lambda}^{\mathbf{i}\Lambda'} = \langle \mathbf{i}\Lambda|V'|k\Lambda'\rangle$ is of crucial importance for the interplay between the one-site crystal-field excitations and the non-local spin liquid excitations (here V' is the component of the crystal field which has a symmetry lower than that diagonalizing the f -electron energy terms E_Γ). Respectively, the non-CC effective exchange constant is introduced as

$$\tilde{J}_{\mathbf{i}}^{\Lambda\Lambda'}(k, k') = \bar{V}_{k\Lambda}^{\mathbf{i}\Lambda'*} V_{k'\Lambda'}^{\mathbf{i}} / (\epsilon_k - E_\Gamma).$$

In the case of completely suppressed charge fluctuations in the f -channel the sf-exchange can be taken into account in the second order approximation, and one comes to the effective RKKY-like Hamiltonian, where the f -electrons

are represented only by their spin degrees of freedom described by the spin-fermion operators $f_{i\Lambda}$. When the CF excitations are involved, this Hamiltonian acquires the following form (detailed derivation of H^s can be found in Refs. [15,23]):

$$H^s = H_f + H_h + H_{RKKY}^{(c)} + H_{RKKY}^{(nc)} . \quad (4)$$

Here

$$H_f = \sum_{i,\Lambda} E_\Gamma |\mathbf{i}\Lambda\rangle \langle \mathbf{i}\Lambda| \quad (5)$$

describes the $Ce(f^1)$ -ions on the lattice sites.

$$H_h = \sum_{\mathbf{i}} \left[\sum_{\Lambda\Lambda'} \mathcal{B}_i^{\Lambda\Lambda'} \delta_{\Lambda\Lambda'} f_{i\Lambda}^\dagger f_{i\Lambda} + \tilde{\mathcal{B}}_i^{\Lambda\Lambda'} f_{i\Lambda}^\dagger f_{i\Lambda'} (1 - \delta_{\Lambda\Lambda'}) \right] \quad (6)$$

corresponds to effective covalent contribution to the one-site CF splitting due to virtual sf-transitions. Here

$$\mathcal{B}_i^{\Lambda\Lambda} = - \sum_{\mathbf{k}} \frac{\bar{V}_{k\Lambda}^{i*} V_{k\Lambda}^i}{\epsilon_k - E_\Gamma}, \quad \tilde{\mathcal{B}}_i^{\Lambda\Lambda'} = - \sum_{\mathbf{k}} \frac{\bar{V}_{k\Lambda}^{i*} V_{k\Lambda'}^i}{\epsilon_k - E_\Gamma} .$$

The effective exchange interaction mediated by conduction electrons is given by the last two terms in the Hamiltonian (4)

$$H_{RKKY}^{(c)} = \sum_{\mathbf{ii}'} \sum_{\Lambda\Lambda'} \mathcal{I}_{\mathbf{ii}'}^{\Lambda\Lambda'} f_{i\Lambda}^\dagger f_{i\Lambda'} f_{i'\Lambda'}^\dagger f_{i'\Lambda} , \quad (7)$$

and the non-CC interaction is represented by the last term $H_{RKKY}^{(nc)}$ which is responsible for the interplay between the HF and CF excitations in our model,

$$H_{RKKY}^{(nc)} = \sum_{\mathbf{ii}'} \sum_{\substack{\Lambda \neq \Lambda'' \\ \Lambda\Lambda'\Lambda''}} \left[\bar{\mathcal{I}}_{\mathbf{ii}'}^{\Lambda\Lambda'\Lambda''} f_{i\Lambda}^\dagger f_{i\Lambda'} f_{i'\Lambda'}^\dagger f_{i'\Lambda''} + H.c. \right] . \quad (8)$$

This is the lowest in \bar{V}_k term among the non-CC indirect exchange interactions which admix the excited CF states $|\Lambda\rangle = |E\nu'\rangle$ to the ground state doublet $|\Lambda\rangle = |G\nu\rangle$.

The uniform spin-liquid state in the Heisenberg-like Hamiltonians with antiferromagnetic exchange constant is described by the free energy expression

$$\mathcal{F} = \beta^{-1} \int_0^{\beta^{-1}} \mathcal{E}(\beta') d\beta' - \beta^{-1} \mathcal{S}_\infty \quad (9)$$

where $\beta^{-1} = k_B T$, \mathcal{S}_∞ is the magnetic entropy at $T \rightarrow \infty$, and \mathcal{E} is the average value of the Hamiltonian expressed via the two-spinon correlator. In the case of the isotropic Heisenberg Hamiltonian this average energy is given by

$$\mathcal{E} = \sum_{\mathbf{ii}'} \frac{\mathcal{I}_{\mathbf{ii}'}}{2} \langle |\Delta_{\mathbf{ii}'}|^2 \rangle \quad (10)$$

where

$$\Delta_{\mathbf{ii}'} = \sum_{\alpha} f_{i\alpha}^\dagger f_{i'\alpha} \quad (11)$$

is the non-local operator creating the RVB pair, α stands for the "flavor" (e.g., spin projection in case of pure spin states). After Fourier transformation the average energy of the uniform spin liquid acquires the form

$$\mathcal{E} = \frac{\mathcal{I}}{2} \sum_{\mathbf{p}\mathbf{q}} \sum_{\alpha\alpha'} \varphi_{\mathbf{p}-\mathbf{q}} \langle \Delta_{\mathbf{p}} \Delta_{\mathbf{q}} \rangle . \quad (12)$$

Here $\varphi_{\mathbf{k}} = \sum_n \exp(-i\mathbf{k}\mathbf{R}_n)$ is the structure factor for the exchange interaction.

Usually, in 3D Heisenberg lattices the spin liquid state has higher energy than the AFM state [24], and the standard mean field approach predicts magnetic order at low temperatures. However, the mechanism stabilizing the spin liquid state in Kondo lattices was proposed in Refs. [16,25]. It was shown within the mean-field approximation that the AFM phase can be suppressed by Kondo-type screening, provided $\mathcal{I} \sim k_B T_K$, and that the spin-liquid state which is not that sensitive to Kondo scattering can be realized instead. Recently it was pointed out [26] that the influence of low-lying relaxation modes in the spin system can transform the phase transition to the spin liquid state into a crossover. The low-lying excitation mode (in particular, the soft CF excitations) can play a similar role in stabilization of the spin liquid state, and the thermodynamics in this case should be described by the equation generalizing eq. (12) for the case of CF excitations admixed to the ground Kramers state of the rare-earth ion. The dynamical correlation function $\langle \Delta_{\mathbf{p}} \Delta_{\mathbf{q}} \rangle_{\omega}$ determines the frequency dependence of inelastic magnetic neutron scattering [15], so the possibility opens for a unified description of low-temperature thermodynamics and the low-energy spin excitations.

To realize this possibility we first should derive the expression for the free energy of the Kondo lattice described by the Hamiltonian H^s (4). This means that we should find the energy \mathcal{E} or, eventually, to diagonalize the matrix

$$\mathbf{M} = \mathbf{H}^s - 1 \cdot \mathbf{E} \quad (13)$$

in terms of the variables Δ .

Having in mind the low symmetry of the CeNiSn lattice, we consider the general case of the elementary cell \mathbf{I} containing several sublattices $\xi = 1, \dots, L$ possessing the same point symmetry group as the Ce ion which total magnetic moment is $J = 5/2$. When diagonalizing $\langle H^s \rangle$ given by eq. (4) in terms of spin liquid variables, we introduce a single anomalous correlator $\Delta^G = \langle f_{V\xi G}^\dagger f_{I\xi G} \rangle$, which corresponds to the ground state doublet $\Lambda = G$. In the course of the diagonalization procedure it turns out that this parameter determines the dispersion of both the lower and the higher branches of the excitation spectrum which arise due to interplay between CF and HF excitations (see Appendix A).

We introduce the Fourier transformation

$$f_{I\xi\Lambda}^\dagger = N^{-1/2} \sum_{\mathbf{k}\nu} e^{i\mathbf{k}\mathbf{l}} \Theta_\nu^\Lambda(\xi, \mathbf{k}) f_{\mathbf{k}\nu}^\dagger \quad (14)$$

to the basis $\{\mathbf{k}\nu\}$ which diagonalizes the translationally invariant matrix \mathbf{M} (eq. 13) and the averages $\langle f_{V\xi\Lambda}^\dagger f_{I\xi\Lambda} \rangle$ ($\nu = 1, \dots, (2J+1)L$). The eigenvectors Θ_ν^Λ are orthonormal,

$$\begin{aligned} \sum_{\nu} \Theta_\nu^\Lambda(\xi, \mathbf{k}) [\Theta_{\nu'}^{\Lambda'}(\xi', \mathbf{k})]^* &= \delta_{\Lambda\Lambda'} \delta_{\xi\xi'}, \\ \sum_{\Lambda\xi} \Theta_\nu^\Lambda(\xi, \mathbf{k}) [\Theta_{\nu'}^{\Lambda'}(\xi, \mathbf{k})]^* &= \delta_{\nu\nu'} \quad . \end{aligned} \quad (15)$$

As a result, the average energy becomes the functional of the "occupation numbers"

$$\langle f_{\mathbf{k}\nu}^\dagger f_{\mathbf{k}'\nu'} \rangle = n_{\mathbf{k}\nu} \delta_{\mathbf{k}\mathbf{k}'} \delta_{\nu\nu'} \quad , \quad (16)$$

and the final equation for energy per Ce ion $\mathcal{E}(T, \{n_{\mathbf{k}}\})$ has the form

$$\mathcal{E}(T, \{n_{\mathbf{k}}\}) = \frac{\Delta_{CF}^{(0)}}{NL} \sum_{\mathbf{k}\nu} n_{\mathbf{k}\nu} \Phi_{\mathbf{k}\nu}(\{n_{\mathbf{k}}\}) \quad (17)$$

(see Appendix B). Here $\Delta_{CF}^{(0)}$ is the energy of the lowest CF excitation which is introduced for the sake of convenience to make all matrices dimensionless), $\{n_{\mathbf{k}\nu}\}$ is the set of average occupation numbers $n_{\mathbf{k}\nu}$ which obeys the mean-field global constraint condition

$$N^{-1} \sum_{\mathbf{k}\nu} n_{\mathbf{k}\nu} = 1 \quad . \quad (18)$$

The occupation numbers

$$n_{\mathbf{k}\nu} = \left[1 + \exp \left\{ \frac{\Delta_{CF}^{(0)} \Phi_{\mathbf{k}\nu} - \mu}{k_B T} \right\} \right]^{-1} \quad (19)$$

are defined in terms of form factors $\Phi_{\mathbf{k}\nu}$

$$\Phi_{\mathbf{k}\nu} = \sum_{\xi\xi'} \sum_{\Lambda\Lambda'} \Theta_{\nu}^{\Lambda}(\xi, \mathbf{k}) \mathcal{Z}_{\xi\xi'}^{\Lambda\Lambda'}(\mathbf{k}) \left[\Theta_{\nu}^{\Lambda'}(\xi', \mathbf{k}) \right]^* . \quad (20)$$

(μ is the chemical potential). Then the matrix \mathbf{Z} represented by its matrix elements

$$\mathcal{Z}_{\xi\xi'}^{\Lambda\Lambda'}(\mathbf{k}) = F^{\Lambda\Lambda'} \delta_{\xi\xi'} + \frac{1}{2} \sum_{\mathbf{u}} e^{i\mathbf{k}\mathbf{u}} \Delta_{\xi\xi'}^{\Lambda\Lambda'}(\mathbf{u}), \quad (21)$$

should be diagonalized to find the eigenvectors $\Theta_{\nu}^{\Lambda}(\xi, \mathbf{k})$. Here $\mathbf{u} = \mathbf{1} - \mathbf{l}'$. The matrix $F^{\Lambda\Lambda'}$ has the form

$$F^{\Lambda\Lambda'} = \delta_{\Lambda\Lambda'} \left(E_{\Lambda} + \mathcal{B}^{\Lambda\Lambda} + \sum_{\mathbf{l}'\xi'} I_{\xi\xi'}^{\Lambda}(\mathbf{1} - \mathbf{l}') \Delta_{CF}^{(0)} \right) / \Delta_{CF}^{(0)} + \mathcal{B}^{\Lambda\Lambda'} / \Delta_{CF}^{(0)} \quad (22)$$

($I_{\xi\xi'}^{\Lambda}(\mathbf{1} - \mathbf{l}')$ is the dimensionless exchange integral, see Appendix A.) Finally, the variables $\Delta_{\xi\xi'}^{\Lambda\Lambda'}(\mathbf{u})$ describing the RVB state [cf. eq. (11)] are to be obtained self-consistently from the system of equations (69).

Thus, to calculate the thermodynamic coefficients of CeNiSn we use the following procedure.

(i) We find the eigenstates $\varepsilon_{\mathbf{k}\nu}$ of the matrix $\Phi_{\mathbf{k}\nu}$ which depend on the parameters of the Hamiltonian H^s .

(ii) These eigenstates are used to calculate the imaginary part of the correlation function $\mathcal{K}(\mathbf{Q}, \omega) = \langle \mathbf{J}_{\mathbf{Q}} \mathbf{J}_{-\mathbf{Q}} \rangle_{\omega}$ which determines the dynamic magnetic response of the system,

$$\text{Im} \mathcal{K}^{\alpha\beta}(\mathbf{Q}, \omega) = \sum_{\nu\nu'} \sum_{\mathbf{k}} n_{\mathbf{k}\nu} (1 - n_{\mathbf{k}-\mathbf{Q},\nu'}) \langle \mathbf{k}\nu | \hat{\mathbf{J}}_{\alpha}^{+} | \mathbf{k} + \mathbf{Q}, \nu' \rangle \langle \mathbf{k} + \mathbf{Q}, \nu' | \hat{\mathbf{J}}_{\beta} | \mathbf{k}\nu \rangle \delta(\hbar\omega + E_{\mathbf{k}\nu} - E_{\mathbf{k}+\mathbf{Q},\nu'}) \quad (23)$$

and, therefore, scattering function of magnetic neutron scattering [15].

(iii) The average energy \mathcal{E} is determined by the Fourier component of this correlation function taken at zero moment

$$\mathcal{K}_{\mathbf{Q}}^{(0)} = \int d\mathbf{k} d\omega \mathcal{K}^{\alpha\beta}(\mathbf{k}, \mathbf{Q}, \omega) \quad (24)$$

(see eq. 12 and Appendix B). Being diagonalized in terms of the eigenstates $|\mathbf{k}\nu\rangle$, this energy is given by eq. (17).

(iv) Then, using experimental results of neutron scattering and thermodynamic measurements we fit the model parameters to describe the neutron scattering function in absolute units and the heat capacity. Since the heat capacity, unlike the neutron scattering spectra, is sample dependent we obtained two set of parameters. The first set describes the data for high quality samples and the second one corresponds to the sample used in dilatometric measurements.

The uniform static susceptibility $\chi(T)$ characterizes the thermodynamic response to an external magnetic field and its volume dependence (magnetostriction is determined by the limiting value of $\mathcal{K}(0, 0)$). We calculate it from the relation $\chi(T) = M/B$ where B is magnetic field, and M is the magnetization of the spin liquid. Only the Zeeman mechanism of this magnetization is taken into account in the case of weak fields ($\mu_B B$ less than the characteristic coupling parameters which determine the spin-fermion spectrum).

IV. THERMODYNAMIC RELATIONS

We suppose that the low-temperature thermodynamics of CeNiSn is determined mainly by the spin-liquid excitations. Since the spin liquid is an unconventional Fermi liquid, and since our treatment of the spin-liquid state inherits some of the shortcomings of the mean-field approximation, we start the discussion of the thermodynamic relations with a more detailed analysis of spin entropy. It is well known [27] that one should take special precautions to eliminate the unphysical states when introducing the fermionic representation for the spin operators (e.g., the states doubly occupied by fermions with opposite spin projections which are absent in original spin representation should be excluded). Without such exclusion the wrong temperature behavior of entropy $S(T)$ will result in incorrect description of the specific heat and other coefficients which are connected with the specific heat by strict thermodynamical relations.

To verify the applicability of our approach we compared the number of states in our model with that in the usual Fermi liquid. The model situations considered in Appendix B demonstrate non-universality of the $S(T)$ law

and its crucial dependence on the parameters of the Hamiltonian, and, in particular, on the character of admixing the magnetic CF excitations to the lowest Kramers doublet in the course of forming the spin-fermion branch of the excitation spectrum. The diagonalization procedure described above gives the equation for the average energy which is sensitive both to the degeneracies of the bare states of the Hamiltonian H_f which are lifted by the spin-liquid correlations, and to the temperature compared with the degeneracies lifted already in H_f (CF level splitting). According to the calculations for the third model of Appendix B which is close enough to the real situation in CeNiSn (see below) the average energy of the spin liquid (17) in the Kondo lattice with several sublattices and several Kramers doublets involved can be presented in the form

$$\mathcal{E}(T) = \frac{\Delta_{CF}^{(0)}}{NL} \frac{1}{2} \kappa(T) \sum_{\mathbf{k}\nu} n_{\mathbf{k}\nu} \varepsilon_{\mathbf{k}\nu}(\{n_{\mathbf{k}}\}) \quad (25)$$

where $\Delta_{CF}^{(0)} = E_E - E_G$, and the factor $\frac{1}{2}\kappa(T)$ reflects the abovementioned fundamental difference between the spin-fermion state and the conventional Fermi liquid.

This factor is essentially nonuniversal: it depends both on the degeneracy of the low-energy branches and the lattice geometry. We simplify our consideration by adopting a single value of this parameter for a given geometry of the lattice and given set of model Hamiltonian parameters. As is shown in Appendix B, the main quantity which predetermines the effective value of κ at low temperatures, $k_b T \ll \Delta_{CF}^{(0)}$, is the degeneracy lifted by spin liquid correlations. According to the results of description of the neutron scattering spectra in CeNiSn [15], the "hidden" degeneracy of the spectrum equals 4 because (i) all Ce ions are in equivalent crystallographic positions, (ii) the mixing interactions comparable in magnitude with $\Delta_{CF}^{(0)}$ connects only Ce ions belonging to the same bc -planes (see fig. 4) although the CeNiSn lattice formally has four sublattices, (iii) only one excited state $|E\pm\rangle = |\pm 3/2\rangle$ interplays with the ground state $|G\pm\rangle = |a|\pm 1/2\rangle \pm |b|\mp 5/2\rangle$ which is responsible for the formation of the spin-fermion branch of the spectrum. As a result we come to the situation with two Kramers doublets and two sublattices which is treated in details in the last example of Appendix B. Therefore we adopt the value of $\kappa = 1/4$ at $k_b T \ll \Delta_{CF}^{(0)}$.

At high temperatures the admixing of higher states (the magnetic CF excitons and the branches split due to inter-sublattice exchange) becomes essential. As a result, the estimations of the coefficients in equation (82) together with the normalization condition (15) give the value of $\kappa \approx 1/2$ for these temperatures. Eventually, at high enough temperatures exceeding all energy splittings in our Kondo lattice the normal behavior $\mathcal{S}(T)$ is restored, but the apparent [28] entropy deficit at low and intermediate temperatures is an intrinsic property of the model. This deficit is an observable effect and its existence was noticed in many measurements (see below).

The spinon contribution to the heat capacity $c_V(T)$ per mole of Ce ion for fixed volume V was calculated using the standard expression

$$c_V(T) = N_A (\partial \mathcal{E}(T) / \partial T)_V \quad (26)$$

where $\mathcal{E}(T)$ is the spinon energy per magnetic ion (25) and N_A is the Avogadro number. The molar spinon entropy for fixed volume \mathcal{S}_m and the free energy of the mole $\mathcal{F}_m(T)$ are found from equations

$$\mathcal{S}_m(T) = \int_0^T \frac{c_V(\tau)}{\tau} d\tau, \quad (27)$$

$$\mathcal{F}_m(T) = N_A \mathcal{E}(T) - T \mathcal{S}_m(T). \quad (28)$$

It is known that, in general, such thermodynamic characteristics as the magnetic susceptibility, the volume expansion coefficient and the volume magnetostriction can be estimated from the dependence of free energy $\mathcal{F}_m(T, V, B)$ on the volume V and magnetic field B . We find these dependences within a framework of the model of spinon spectrum which was successfully used in [18] for the description of inelastic neutron scattering spectrum.

V. MODEL OF SPINON SPECTRUM

CeNiSn crystallizes in the orthorhombic lattice which belongs to the noncentrosymmetric space group $Pn2_1a$ [29]. The point symmetry of the crystal field on Ce ions can be treated as nearly trigonal (D_{3d}) with the rotation axis parallel to the a -axis of the crystal, and the monoclinic distortion (C_s) can be considered as a small correction to the trigonal crystal field [14]. Therefore, to describe the bare CF states Λ we use the irreducible representation of the trigonal point group D_{3d} . It is shown by indirect experiments [14] and confirmed by the quantitative agreement

of the calculated and experimental inelastic neutron scattering spectra [15] that the ground state level and the first excited level form a pair of Kramers doublets

$$|G\pm\rangle = a|\pm 1/2\rangle \pm b|\mp 5/2\rangle, \quad (29)$$

$$|E\pm\rangle = |\pm 3/2\rangle \quad (30)$$

separated by the energy interval $\Delta_{CF} < 40K$ which is much less than the energy of the second excited CF level of Ce $\Delta_{CF}^{(2)}$. The recently reported excitations centered around 40 meV [30], apparently should be ascribed to this second CF state.

To calculate the average energy $\mathcal{E}(T)$ one should solve the system of equations (20,21,22,69) under the constraint (18). We are interested in the low-T thermodynamics of CeNiSn, ($T < 20K$). These temperatures are essentially less than the bandwidth of the RVB band ($W \approx 150K$, see [15]), so we can treat approximately the anomalous averages Δ^{GG} as temperature independent correlators [31,32].

It was shown in [15] that the interactions which form the dispersion of the spin liquid excitations are confined mainly within the bc plane of the CeNiSn lattice. The structure of this plane is determined by the orthorhombic 2D elementary cells which contain two Ce ions in the sites $\mathbf{i} = \mathbf{l}\xi$ where $\xi = 1, 2$ is the sublattice index (see fig. 4). This network is defined by the Bravais vectors $\mathbf{B} = (b, 0)$ and $\mathbf{C} = (0, c)$ and the basis vector $\mathbf{d} = (0, -b/2, c/2 - \mathcal{O})$. Here \mathcal{O} is the orthorhombic distortion which transforms the one-ion hexagonal lattice into the two-ion orthorhombic one.

To describe the 2D spinon spectrum *at low temperatures* $T \rightarrow 0$ one has to introduce the coupling constants which describe the matrix $Z_{\xi\xi'}^{\Lambda\Lambda'}(\mathbf{k})$ (21). We confine ourselves with the simplest nearest neighbours (nn) approximation and introduce the parameters $\mathcal{T}_{\mathbf{i}\mathbf{i}'}$ which describe the in-sublattice

$$\mathcal{T}_1 = \Delta_{CF}^{(0)}\Delta_{11}^{GG}(nn)/2 = \Delta_{CF}^{(0)}\Delta_{22}^{GG}(nn)/2 \quad (31)$$

and inter-sublattice

$$\mathcal{T}_2 = \Delta_{CF}^{(0)}\Delta_{12}^{GG}(nn)/2 = \Delta_{CF}^{(0)}\Delta_{21}^{GG}(nn)/2 \quad (32)$$

coupling. These constants are responsible for the formation of the spinon spectrum which arise due to RVB correlations within the ground state CF level $\Lambda = G$ [15]. Similarly, the interplay of spinons with the lowest excited CF state $\Lambda = E$ is defined by the intra-site nondiagonal matrix element given by eq. (22)

$$\mathcal{G}_1 = F^{GE} = F^{EG} \quad (33)$$

and the inter-site mixing coefficient

$$\mathcal{G}_2 = \Delta_{CF}^{(0)}\Delta_{\xi\xi'}^{GE}(nn)/2 = \Delta_{CF}^{(0)}\Delta_{\xi\xi'}^{EG}(nn)/2; \xi \neq \xi' \quad (34)$$

The condition $\xi \neq \xi'$ for intermixing of ground and excited doublets arises due to the orthorhombic distortion which results in the two-sublattice structure of the plane (Fig. 4).

To introduce the renormalised CF splitting $\tilde{\Delta}_{CF}$ one has to consider the diagonal terms of eq. (22). This contribution

$$\tilde{\Delta}_{CF} = \Delta_{CF}^{(0)}(F^{EE} - F^{GG}) \quad (35)$$

renormalises the bare value of CF splitting $\Delta_{CF}^{(0)} = E_E - E_G$. Then two terms determine the renormalization of CF splitting Δ_{CF}^0

$$\tilde{\Delta}_{CF} = \Delta_{CF}^{(0)} + \delta_1 + \delta_2. \quad (36)$$

The first correction

$$\delta_1 = \mathcal{B}^{EE} - \mathcal{B}^{GG}, \quad (37)$$

is defined by intra-site processes, and the second one is due to inter-site interaction

$$\delta_2 = \sum_{\mathbf{l}'\xi'} \{ I_{\xi\xi'}^E(\mathbf{l} - \mathbf{l}') - I_{\xi\xi'}^G(\mathbf{l} - \mathbf{l}') \}. \quad (38)$$

Details of the procedure which diagonalizes the matrix $Z_{\xi\xi'}^{\Lambda\Lambda'}(\mathbf{k})$ and gives the eigenvectors $\Theta_{\nu}^{\Lambda}(\xi, \mathbf{k})$ and eigenvalues $\Phi_{\mathbf{k}\nu}$ are described in [15].

VI. SAMPLE DEPENDENCE OF THERMODYNAMIC PROPERTIES

It is known that the thermodynamic properties of CeNiSn depend on the specimen quality [33]. At the same time the main features of inelastic magnetic scattering spectra are the same (i.e. 2.5 meV and 4 meV inelastic excitations) for different specimens [7,8,34]. Therefore, the theory which consider the thermodynamics should explain both the sample dependent thermodynamic properties and the sample independent neutron scattering function.

First, it is known that the more imperfect is the sample of CeNiSn, the higher is the residual resistivity [5] and the lesser is the mean free path of the electrons λ . The increase of λ in more perfect crystals results in the decrease of the exchange RKKY-type interaction $I(R_{\text{Ce-Ce}}) \sim \exp(-R_{\text{Ce-Ce}}/\lambda)$ [35] which determines the parameters \mathcal{T}_1 and \mathcal{T}_2 . Therefore these parameters should be smaller for less perfect samples. Moreover, since the relative change of the resistivity is higher along the c -axis than along the b -axis, the suppression of the exchange interaction along the c -axis should be larger. Hence, the reduction of \mathcal{T}_2 is greater than that of \mathcal{T}_1 .

Second, the increase of the defect concentration results in the increase of the inter-site mixing parameter \mathcal{G}_1 due to lowering of the lattice symmetry. The change of the inter-site mixing parameter \mathcal{G}_2 is influenced both by increase of defect induced mixing and by reduction of inter-site exchange. Therefore, the influence of imperfections on this parameter is not known a priori. Since it is supposed [15] that $|I_{\xi\xi'}^G(\mathbf{1}-\mathbf{1}')| \gg |I_{\xi\xi'}^E(\mathbf{1}-\mathbf{1}')|$, the renormalisation of CF splitting $\tilde{\Delta}_{CF} - \Delta_{CF}^{(0)}$ is defined mainly by the exchange interaction $I_{\xi\xi'}^G(\mathbf{1}-\mathbf{1}')$. One of the conditions of spin liquid RVB state formation is the positive antiferromagnetic sign of these interactions. Therefore, the renormalised value of CF $\tilde{\Delta}_{CF}$ is lower for better samples.

The last effect which has to be considered is the change of the coefficients of the wave functions (29). This change is connected with the renormalization of the wave functions of low-symmetry system when the exchange interaction changes [36].

Two sets of parameters which take into account these tendencies for the high quality specimen [5] and the specimen which was used in linear expansion and magnetostriction measurements [13,17] are presented in Table 1. The fragments of DOS for both sets of parameters are shown in Fig. 5. The heat capacity for perfect and imperfect specimens are presented in Fig. 6. To illustrate the relative insensibility of neutron spectra to the sample quality we calculated the scattering function (in absolute units) for momentum transfers where 2.5 meV (Fig. 7a) and 4 meV (Fig. 7b) are observed. It is seen that the neutron scattering spectra for both specimens coincide in gross features. The experimental absolute values [8] of the scattering cross sections are also reproduced. More detailed description of the influence of sample quality on the properties of CeNiSn will be presented in a forthcoming publication.

In the following analysis we use the set of parameters presented in the second column of Table 1 which correspond to the heat capacity of the less perfect specimen used in dilatometric measurements [13,17].

VII. MAGNETIC SUSCEPTIBILITY

The standard definition

$$\chi_m(T) = -\frac{1}{B} \left(\frac{\partial \mathcal{F}_m(T)}{\partial B} \right)_{T,N} \quad (39)$$

was used in the calculation of spinon contribution to molar magnetic susceptibility χ_m . Since the magnetic response of CeNiSn is maximal for field B_a applied along a -direction [1], we consider only this easy axis component of χ_m and limit ourselves by Zeeman mechanism of polarization of spin liquid described by the Hamiltonian

$$\hat{H}_Z = g_J \nu_B \hat{J}_a B_a . \quad (40)$$

Here $g_J = 6/7$ is the Lande factor for Ce^{3+} configuration, ν_B is Bohr magneton and \hat{J}_a is the a -projection of total angular momentum operator. It is known [1] that the Sommerfeld coefficient $\gamma_{sp} \equiv C(T)/T$ is practically constant at lowest temperatures $T < 1\text{K}$. Therefore we use the Fermi liquid relations for spinon subsystem at $T \rightarrow 0$. For example, the Wilson ratio for spinon liquid can be derived in close analogy with electron Fermi liquid. expression. The spinon wave function in the band ν with a wave vector \mathbf{k} can be represented as a linear combination

$$|\nu\mathbf{k}\rangle = \sum_{\lambda=1}^6 \mathcal{L}_\lambda(\nu, \mathbf{k}) \left| \frac{2\lambda-7}{2} \right\rangle, \quad (41)$$

where $\mathcal{L}_\lambda(\nu, \mathbf{k})$ are coefficients which obey the orthonormality relations. Therefore, applying the Zeeman operator (40) to this state we calculate the factor G_{sp}

$$G_{sp} = \left(\sum_{\lambda=1}^6 |\mathcal{L}_\lambda(\nu, \mathbf{k})|^2 \frac{2\lambda - 7}{2} \right)^2 \quad (42)$$

which appears in the Wilson ratio instead of the electron g -factor:

$$\chi_m(T \rightarrow 0) = \frac{3}{\pi^2} \frac{\mu_B^2}{k_B^2} G_{sp} \gamma_{sp}. \quad (43)$$

Neglecting in the simplest approximation admixture of the state $|E\pm\rangle = |\pm 3/2\rangle$ to the spinons which form the RVB band, we find that the lowest spinon state generated by the level (29) gives

$$G_{sp} = g_J^2 (5b^2/2 - a^2/2)^2. \quad (44)$$

Then, using the parameters from the last column of table 1, we find the value of $1.34 \cdot 10^{-3}$ emu/mol for the spinon magnetic susceptibility at $T \rightarrow 0$. This calculated value is significantly lower than the measured one. Therefore, one should conclude, that either magnetic susceptibility is determined not only by spinon contribution, or that the mechanism of magnetic field influence on the spin liquid can not be reduced to simple Zeeman splitting.

To resolve this alternative, we calculated the temperature dependence of magnetic susceptibility up to $T = 20\text{K}$ by direct use of eq. (39). It is seen (Fig. 8) that good agreement with experiment can be obtained if one consider the total magnetic susceptibility as a sum of spinon Zeeman part $\chi_{sp}(T)$ and background contribution $\chi_b = 6.35 \cdot 10^{-3}$ emu/mol which is constant at $T < 20\text{K}$. This calculation perfectly reproduces the position of maximum and the shape of the curve at $T < 20\text{K}$. Since $\chi_{sp}(T)$ in this temperature interval is determined by the low-energy sharp features of spinon spectrum one can conclude that the Zeeman splitting of the structured part of spinon spectrum is responsible for observed behavior of $\chi(T)$. The contribution χ_b is, apparently, determined by energy scales which are higher than the CF splitting. Possible sources of this contributions will be discussed in concluding section 9.

It should be noted that the spinon response perfectly reproduces the intensities of the 2.5 meV and 4 meV peaks in the inelastic magnetic scattering spectra of neutrons in *absolute units*. Both peaks are connected with the low energy structured part of spinon spectrum. This observation gives one more evidence in favor of the assumption that the constant contribution to static magnetic susceptibility is connected with larger energy scales.

More evidences in favor of additional contributions to magnetic response are provided by detailed study of thermal expansion and magnetostriction presented in the next section.

VIII. TEMPERATURE AND FIELD DEPENDENCE OF LATTICE DISTORTION

A. Thermal expansion

The conventional phenomenological analysis of the thermal expansion of Kondo lattices is based on the assumption that the characteristic temperature T_K scales all thermodynamic quantities at low T , so the main contribution to the volume dependence of these quantities may be characterized by a Grüneisen parameter $\gamma_{T_K} = \partial \log T_K / \partial \log V$. We have seen that the interplay between heavy fermions and crystal field excitations introduces an additional characteristic energy scale $\tilde{\Delta}_{CF}$ and a corresponding coupling constant, so this interplay rules out a possibility of being content with a single scaling parameter. Moreover, the energy T^* is, apparently, not related directly to T_K in the CeNiSn family. Thus we start this section with the derivation of Grüneisen parameters which characterize the spin liquid in Kondo lattices with soft CF excitations, still confining ourselves to $T \leq \Delta_{CF} \ll T_K$. The volume thermal expansion coefficient

$$\alpha_V = \left(\frac{\partial \log V}{\partial T} \right)_P \quad (45)$$

(P is pressure) can be expressed in terms of the isothermal compressibility $\kappa_T = (\partial \log V / \partial P)_T$ and the isothermal derivative of the total entropy \mathcal{S}_V^{tot} with respect to the volume V [37].

$$\alpha_V = \kappa_T \left(\frac{\partial \mathcal{S}_V^{tot}}{\partial V} \right)_T. \quad (46)$$

Since the Cornut-Coqblin transformation decouples spin and charge degrees of freedom, the total entropy can be expressed as a sum $\mathcal{S}_V^{tot} = \mathcal{S}_V^{sp} + \mathcal{S}_V^{el}$ of the spinon \mathcal{S}_V^{sp} and the conduction electrons \mathcal{S}_V^{el} contribution. The entropy

$\mathcal{S}_V^{el} = V\gamma^{el}T$ of conduction electrons is proportional to the Sommerfeld coefficient γ^{el} at low T , which results in a linear- T law for the thermal expansion

$$\frac{\alpha_V^{el}}{T} = \kappa_T \gamma^{el} \left(1 + \frac{\partial \log \gamma^{el}}{\partial \log V} \right) \quad (47)$$

(see, e.g., [37]).

Due to the inequality $\tilde{\Delta}_{CF} \ll T_K$ the spinon component of α_V^{sp}/T can be decomposed into temperature dependent and constant terms. It is convenient to express the spin entropy and its derivative (46) in molar units,

$$\alpha_V^{sp} = \kappa_T \left(\frac{\partial \mathcal{S}_m}{\partial V} \right)_T. \quad (48)$$

The isothermal compressibility and entropy per mole ($\kappa_T[mJ/mol]$ and $\mathcal{S}_m[mJ/(mol \cdot K)]$) enter this equation. Since the spinon entropy is a function of model constants $\mathcal{P}_i = \tilde{\Delta}_{CF}, \mathcal{T}_1, \mathcal{T}_2, \mathcal{G}_1, \mathcal{G}_2$, one can express its volume derivative in terms of the corresponding Grüneisen parameters.

$$\gamma_i^V = \frac{\partial \log \mathcal{P}_i}{\partial \log V}. \quad (49)$$

Strictly speaking, the volume dependence of $\tilde{\Delta}_{CF}$ has to be expressed in terms of magnetoelastic Hamiltonian constants [38]. However, in case of significant contribution of exchange interaction the standard magnetoelastic Hamiltonian has to be revised [36]. Therefore, we prefer to describe the magnetoelastic coupling in terms of Grüneisen parameters, which reflect the main features of magnetoelastic interaction.

As a result, the spinon contribution to the volume thermal expansion coefficient acquires the form

$$\frac{\alpha_V^{sp}}{T} = \kappa_T \frac{\mathcal{S}_m}{T} \sum_i \gamma_i^V \left(\frac{\partial \log \mathcal{S}_m}{\partial \log \mathcal{P}_i} \right)_T. \quad (50)$$

The peculiar features of α_V^{sp}/T are determined by those terms which demonstrate appreciable temperature dependence of the logarithmic derivatives $\partial \log \mathcal{S}_m / \partial \log \mathcal{P}_i$. The logarithmic derivatives $\partial \log \mathcal{S}_m / \partial \log \mathcal{T}_{1,2}$, which can be expressed in terms of conventional Grüneisen parameter $\gamma_{T_K} = \partial \log T_K / \partial \log V$, are temperature independent in the considered temperature range $T \ll T_K$. Therefore, these terms can be incorporated into a constant W_V together with the temperature independent contribution of conduction electrons

$$W_V = \kappa_T \gamma^{el} \left(1 + \frac{\partial \log \gamma^{el}}{\partial \log V} \right) + \kappa_T \frac{\mathcal{S}_m}{T} \gamma_{T_K}^V \left(\frac{\partial \log \mathcal{S}_m}{\partial \log T_K} \right)_T. \quad (51)$$

Finally we come to the following expression for the volume thermal expansion coefficient

$$\frac{\alpha_V}{T} = W_V + \frac{\kappa_T}{T} \left\{ \gamma_{\tilde{\Delta}_{CF}} \left(\frac{\partial \mathcal{S}_m}{\partial \log \tilde{\Delta}_{CF}} \right)_T + \gamma_{\mathcal{G}_1} \left(\frac{\partial \mathcal{S}_m}{\partial \log \mathcal{G}_1} \right)_T + \gamma_{\mathcal{G}_2} \left(\frac{\partial \mathcal{S}_m}{\partial \log \mathcal{G}_2} \right)_T \right\}. \quad (52)$$

Although one can not distinguish between electron and spinon contribution into the constant term W_V , careful analysis of temperature dependent contributions provides important information about the volume dependence of spinons-CF coupling. It is obvious that the on-site mixing strength \mathcal{G}_1 is the parameter which is less influenced by volume change than the crystal field splitting $\tilde{\Delta}_{CF}$ and the intersite mixing parameter \mathcal{G}_2 . Therefore, one can assume that $\gamma_{\mathcal{G}_1} \sim 0$ and then analyse the thermal expansion in terms of *two Grüneisen parameters*, i.e. $\gamma_{\tilde{\Delta}_{CF}}$ and $\gamma_{\mathcal{G}_2}$. This means that even in the temperature range $T \leq \tilde{\Delta}_{CF}$ there are two mechanisms of the volume dependence of the spinon spectrum. Therefore, one can expect that any attempt to describe the volume-dependent properties of CeNiSn by means of a single Grüneisen parameter will result in the temperature dependence of the latter [19].

Our two-parameter procedure gives good agreement with experimental data [17] for the set of parameters $\gamma_{\tilde{\Delta}_{CF}} = -90$ and $\gamma_{\mathcal{G}_2} = -60$ (see Fig. 9). It should be noted that the signs of both Grüneisen parameters are reasonable, i.e. expansion of the lattice leads to softening of Δ_{CF} and to decrease of intersite mixing parameter \mathcal{G}_2 .

To analyse the anisotropy of thermal expansion one has to introduce the axis-dependent Grüneisen parameters

$$\gamma_{\tilde{\Delta}_{CF}}^{x_j} = \frac{\partial \log \tilde{\Delta}_{CF}}{\partial \log x_j}; \quad x_j = a, b, c \quad (53)$$

and

$$\gamma_{\mathcal{G}_2}^{x_j} = \frac{\partial \log \mathcal{G}_1}{\partial \log x_j}; \quad x_j = a, b, c \quad (54)$$

with the obvious property

$$\gamma_i^V = \sum_{x_j}^{a,b,c} \gamma_i^{x_j}; \quad i = \tilde{\Delta}_{CF}, \mathcal{G}_1. \quad (55)$$

A comparison of the calculated linear expansion coefficients with experimental data [13] is presented in Fig. 10. Since the intersite mixing parameter \mathcal{G}_2 can be attributed to the deviation of Ce sublattice symmetry from hexagonal one, one can expect that the magnitude of intersite mixing should be proportional to orthorhombic distortion of Ce sublattice (see, e.g., Fig. 1 in [15]). Therefore, since the lattice expansion along the c -axis is most sensitive to the orthorhombic distortion, the inequality $|\gamma_{\mathcal{G}_2}^c| \gg |\gamma_{\mathcal{G}_2}^{a,b}|$ should be valid. Indeed, the best fit is obtained for $\gamma_{\mathcal{G}_2}^c = -60$ and $\gamma_{\mathcal{G}_2}^b = \gamma_{\mathcal{G}_2}^a = 0$. The same reasoning leads to conclusion about opposite signs of the influence of expansion in the ab plane and along the c axis on the CF parameters. Indeed, the values of fitted Grüneisen parameters are $\gamma_{\tilde{\Delta}_{CF}}^a = -60$, $\gamma_{\tilde{\Delta}_{CF}}^b = -84$ and $\gamma_{\tilde{\Delta}_{CF}}^c = 54$.

B. Magnetostriction

Two-parameter Grüneisen analysis of thermal expansion can be used as the basis for quantitative explanation of the magnetostriction which in our model is the quantity characterising the sensitivity of spinon-CF interplay parameters to the volume change. Reversible volume magnetostriction is thermodynamically equivalent to the strain dependence of the magnetic susceptibility $\chi(B, T)$ [20]

$$\lambda'_V(B, T) = \kappa_T H \chi(B, T) \left(\frac{\partial \log \chi(B, T)}{\partial \log V} \right)_T. \quad (56)$$

Like the thermal expansion, λ'_V in low magnetic fields can be decomposed in the sum of electronic $\lambda'_{V,el}$ and spinon contribution $\lambda'_{V,sp}$

$$\lambda'_V = \lambda'_{V,el} + \lambda'_{V,sp}. \quad (57)$$

The contribution of conduction electrons is temperature independent and linear in magnetic field for $k_B T \ll \varepsilon_F$ and $\nu_B H \ll \varepsilon_F$.

$$\lambda'_{V,el} = \kappa_T W_V^{el} B \quad (58)$$

where

$$W_V^{el} = \left(\frac{\partial \chi_P}{\partial \log V} \right)_T \quad (59)$$

(here χ_p is the Pauli paramagnetic susceptibility). Therefore, to reveal peculiar features of the differential magnetostriction it is convenient to compare experimental and theoretical results for the doubly differential magnetostriction coefficient

$$\lambda''_V = \frac{\lambda'_V}{B} \quad (60)$$

which does not depend on temperature and field in the conventional Fermi liquid. This quantity, is proportional to the volume derivative of the magnetic susceptibility (provided the field and the temperature dependence of the isothermal compressibility is neglected).

The Grüneisen analysis of the magnetostriction is similar to that of the linear expansion. One should take into account only Grüneisen parameters for which the logarithmic derivative of the magnetic susceptibility demonstrates sharp temperature and field dependence whereas the structureless contribution due to the standard Grüneisen parameter γ_{T_K} can be taken into account by the renormalization of the normal Fermi-liquid contribution constant W_V^{el}

→ \tilde{W}_V . However, in addition to the parameters $\gamma_{\mathcal{G}_2}$ and $\gamma_{\tilde{\Delta}_{CF}}$ one should take into account the volume dependence of the coefficient a in the wave function $|G\pm\rangle$ (29)

$$\gamma_a = \frac{\partial \log a}{\partial \log V}. \quad (61)$$

Then the final expression for the logarithmic derivative of the magnetic susceptibility acquires the form

$$\frac{\partial \chi}{\partial \log V} = \tilde{W}_V + \left\{ \gamma_{\tilde{\Delta}_{CF}} \left(\frac{\partial \chi_m}{\partial \log \tilde{\Delta}_{CF}} \right)_T + \gamma_{\mathcal{G}_2} \left(\frac{\partial \chi_m}{\partial \log \mathcal{G}_2} \right)_T + \gamma_a \left(\frac{\partial \chi_m}{\partial \log a} \right)_T \right\} \quad (62)$$

where \tilde{W}_V incorporates all contributions, which are temperature independent at $T < 20\text{K}$

$$\tilde{W}_V = W_V^{el} + \gamma_{T_K} \left(\frac{\partial \chi_m}{\partial \log T_K} \right) \quad (63)$$

The logarithmic derivatives of the magnetic susceptibility are presented in Fig. 11. The fit of the temperature dependence of the volume magnetostriction with $\gamma_{\tilde{\Delta}_{CF}}$ and γ_g found above, $\tilde{W} = -1590 \cdot 10^{-3} \text{emu/mol}$, and $\gamma_a = 230$ gives a reasonable agreement with experimental data at low magnetic fields (Fig. 12). It turns out that the last term of eq. (62) dominates in magnetostriction because the contribution of the first two terms gives a value which is significantly smaller than the experimental data.

Like in case of the magnetic susceptibility, there is a large constant contribution in addition to the temperature dependent term, which may be ascribed to the excitations with the energy scale essentially exceeding that of the structured part of the spinon spectrum. Moreover, this background, which is present both in magnetic susceptibility and magnetostriction, does not appear in linear expansion in zero magnetic field.

It should be mentioned that the suggested analysis is successful only at low magnetic fields. Meanwhile, the field dependence of the magnetostriction yields evidence in favor of a non-Zeeman influence of the magnetic field on the spinon spectrum. The experiments in higher fields give almost temperature independent behavior of the logarithmic derivative of the magnetic susceptibility (see Fig. 3) whereas the Zeeman term behaves similarly both in low and high fields.

IX. CONCLUSION

The theory of spin liquid origin of the low temperature anomalies in thermodynamical and magnetic properties of CeNiSn and related compounds offered in [12,13] is based on the assumption that the pseudogap features of these properties should be ascribed to spin excitations rather than to a non-metallic electron spectrum. Later on, this suspicion was confirmed by metallic-like behavior of the resistivity in samples of good enough quality [5]. Nevertheless, the spin-liquid theory met the challenge of explaining not only the low-temperature thermodynamics but also the fascinatingly complicated picture of inelastic neutron spectra. Explanation of the mechanism of neutron scattering offered in [15] provided us with a set of parameters which determine the spinon spectrum. Thus we came to the quantitative picture of a spin liquid which arises as a result of the interplay between intersite resonating valence bonds (spinons) and one-site crystal field excitations. In the present paper the experimental data on volume-dependent thermodynamical properties of CeNiSn are collected and the quantitative theory of spin liquid is used for interpretation of these data.

To summarize the results of the realization of the above program, one should conclude that the hypothesis that the nonlocal spinon pairs determine the free energy of CeNiSn in accordance with eq. (9) is confirmed by detailed quantitative consideration. These pairs, apparently, are responsible both for the structure of low-energy excitations which determine the spectrum of inelastic neutron scattering, and for the low-temperature thermodynamics (specific heat, thermal expansion). As to magnetic properties (susceptibility, magnetostriction), the real situation is, apparently, more complicated than the picture given by the mean-field version of spin-liquid theory. We confined ourselves by considering the Zeeman polarization of spinon excitations. This mechanism successfully describes the temperature dependences $\chi(T)$ and $\chi'(T)$ at low enough T where the spinon excitations are still well defined. It fails, however, to give the absolute values of these quantities. Besides, the properties of CeNiSn change radically in strong enough magnetic field, and this change is also beyond the applicability of our theory.

At this stage we can only speculate about the presence of another energy scale in the excitation spectrum of the spin liquid. To explain the origin of this high-energy scale one should remember that the *coherent* branch of spinon pairs gives only a small contribution to the low-energy part of the spectral density of spin excitations $\mathcal{A}_s(\varepsilon)$. In the

absence of long range order the dominant contribution to $\mathcal{A}_s(\varepsilon)$ is given by the incoherent structureless continuum of paramagnetic spin fluctuations. The closest analogy to our case is the structure of spin-fluctuation spectrum in Cu-O planes of high- T_c materials described by the $t - J$ model at small doping limit [39,40]. In that model the coherent branch of Zhang-Rice spinon-holon compound particles forms the low-energy part of the spin-polaron continuum. This branch gives a small contribution to $\mathcal{A}_s(\varepsilon)$ with characteristic energy scale J , whereas the main part of $\mathcal{A}_s(\varepsilon)$ is formed by the incoherent structureless spin-polaron continuum scaled by the energy $t \gg J$. Our crude enough mean-field approximation for the spinon spectrum ignores the incoherent continuum. Besides, the influence of magnetic field by no means can be reduced to simple polarization of the spin liquid. We hope that the more refined description of spin liquid in Kondo lattices will reveal the real role of both external magnetic field and intrinsic antiferromagnetic fluctuations in the magnetic response of these systems.

X. ACKNOWLEDGEMENTS

The support of NWO (grant 07-30-002) and RFBR (grant 98-02-16730) is acknowledged.

XI. APPENDIX A

To calculate the thermal energy, one should find the thermodynamic average of the sum of Hamiltonians H_h , $H_{(c)}^{RKKY}$ and $H_{(nc)}^{RKKY}$,

$$\mathcal{E}(T) = \mathcal{E}_h(T) + \mathcal{E}_c(T) + \mathcal{E}_{nc}(T) \quad (64)$$

where

$$\mathcal{E}_h(T) = \frac{\Delta_{CF}^{(0)}}{NL} \sum_{\mathbf{l}\xi} \sum_{\Lambda\Lambda'} F^{\Lambda\Lambda'} \langle f_{\mathbf{l}\xi\Lambda}^\dagger f_{\mathbf{l}\xi\Lambda'} \rangle, \quad (65)$$

$$\mathcal{E}_c(T) = \frac{\Delta_{CF}^{(0)}}{NL} \sum'_{\mathbf{l}'\xi\xi'} \sum_{\Lambda} I_{\xi\xi'}^{\Lambda} (\mathbf{1} - \mathbf{l}') \langle f_{\mathbf{l}'\xi\Lambda}^\dagger f_{\mathbf{l}'\xi'\Lambda} \rangle \langle f_{\mathbf{l}'\xi'\Lambda}^\dagger f_{\mathbf{l}'\xi\Lambda} \rangle, \quad (66)$$

$$\begin{aligned} \mathcal{E}_{nc}(T) = & \frac{\Delta_{CF}^{(0)}}{NL} \sum'_{\mathbf{l}'\xi\xi'} \sum_{\Lambda\Lambda'} (1 - \delta_{\Lambda\Lambda'}) \langle f_{\mathbf{l}'\xi\Lambda}^\dagger f_{\mathbf{l}'\xi'\Lambda'} \rangle \times \\ & \left\{ \tilde{I}_{\xi\xi'}^{\Lambda\Lambda'} (\mathbf{1} - \mathbf{l}') \langle f_{\mathbf{l}'\xi'\Lambda'}^\dagger f_{\mathbf{l}'\xi\Lambda} \rangle + \left[\tilde{I}_{\xi'\xi}^{\Lambda'\Lambda} (\mathbf{l}' - \mathbf{1}) \right]^* \langle f_{\mathbf{l}'\xi'\Lambda}^\dagger f_{\mathbf{l}'\xi\Lambda} \rangle \right\}. \end{aligned} \quad (67)$$

Here N is the number of unit cells, primes in the lattice sums mean that the diagonal terms are omitted,

$$I_{\xi\xi'}^{\Lambda} (\mathbf{1} - \mathbf{l}') = \mathcal{I}_{\mathbf{l}'\xi, \mathbf{l}'\xi'}^{\Lambda\Lambda} / \Delta_{CF}^{(0)} \quad I_{\xi\xi'}^{\Lambda\Lambda'} (\mathbf{1} - \mathbf{l}') = \tilde{\mathcal{I}}_{\mathbf{l}'\xi, \mathbf{l}'\xi'}^{\Lambda\Lambda'\Lambda'} / \Delta_{CF}^{(0)}, \quad (68)$$

and the matrix $F^{\Lambda\Lambda'}$ is defined by the equation (22). The quantities $\Delta_{\xi\xi'}^{\Lambda\Lambda'}(\mathbf{u})$ are described by the system of equations

$$\begin{aligned} \Delta_{\xi\xi'}^{\Lambda\Lambda'}(\mathbf{u}) = & 2N^{-1} \sum_{\mathbf{k}\nu} n_{\mathbf{k}\nu} e^{-i\mathbf{k}\mathbf{u}} \left\{ \delta_{\Lambda\Lambda'} I_{\xi\xi'}^{\Lambda}(\mathbf{u}) \Theta_{\nu}^{\Lambda}(\xi', \mathbf{k}) [\Theta_{\nu}^{\Lambda}(\xi, \mathbf{k})]^* + \right. \\ & \left. (1 - \delta_{\Lambda\Lambda'}) \left(\tilde{I}_{\xi\xi'}^{\Lambda\Lambda'}(\mathbf{u}) \Theta_{\nu}^{\Lambda'}(\xi', \mathbf{k}) [\Theta_{\nu}^{\Lambda'}(\xi, \mathbf{k})]^* + \left[\tilde{I}_{\xi'\xi}^{\Lambda'\Lambda}(-\mathbf{u}) \right]^* \Theta_{\nu}^{\Lambda}(\xi', \mathbf{k}) [\Theta_{\nu}^{\Lambda}(\xi, \mathbf{k})]^* \right) \right\}, \end{aligned} \quad (69)$$

and this system together with equations (20), (21) forms the closed set of equations which should be solved self-consistently.

Although in the general case of low-symmetry lattices with anisotropic exchange constants $I_{\xi\xi'}^{\Lambda}(\mathbf{u})$ and $\tilde{I}_{\xi\xi'}^{\Lambda\Lambda'}(\mathbf{u})$, one should introduce several variables $\Delta_{\xi\xi'}(\mathbf{u})$, for the lattices with high enough symmetry one can confine oneself with a single parameter Δ^{GG} which characterises the intersite correlations within the lowest crystal field level.

For example, in Bravais lattices with P nearest neighbours in equivalent positions the set of parameters should be introduced,

$$\Delta^{\Lambda\Lambda'} = \frac{1}{z} \sum_{\mathbf{u}}^{nn} \Delta^{\Lambda\Lambda'}(\mathbf{u}) . \quad (70)$$

However, if only the lowest crystal field states $|G\pm\rangle$ are responsible for the "anomalous" intersite correlations described by the parameter Δ^{GG}

$$\Delta^{GG} = I^G \frac{2}{Nz} \sum_{\mathbf{k}\nu} \varphi_{\mathbf{k}} n_{\mathbf{k}\nu} |\Theta_{\nu}^G(\mathbf{k})|^2 , \quad (71)$$

there is no need in independent nondiagonal variables $\Delta^{G\Lambda}$. All of them can be expressed via Δ^{GG} by means of the factors $q_{\Lambda} = \tilde{I}^{\Lambda G}/I^{\Lambda G} < 1$,

$$\Delta^{\Lambda G} = q_{\Lambda} \Delta^{GG} . \quad (72)$$

Thus, we assume that the symmetry of CeNiSn lattice is high enough to restrict ourself to a single parameter Δ^{GG} which characterises the intersite correlations within the lowest Kramers doublet.

XII. APPENDIX B

First, we demonstrate that the diagonalized form (17) contains the correct number of states, namely $2N$ levels for the simple case of one-sublattice crystal with spins $1/2$ in each site described by the Hamiltonian

$$H^s = \frac{I}{2} \sum_{\mathbf{i}\mathbf{i}'}^{i \neq i'} \sum_{\nu\nu'} f_{i\nu}^{\dagger} f_{i\nu'} f_{i'\nu'}^{\dagger} f_{i'\nu} \quad (73)$$

($\nu = \pm$ are the spin projections). In this case the average energy of the spin liquid state \mathcal{E}_c is given by the equation:

$$\mathcal{E}_c = \frac{I}{2} \sum_{\mathbf{ij}} \langle b_{\mathbf{ij}} b_{\mathbf{ji}} \rangle = \frac{I}{2z} \sum_{\mathbf{p}\mathbf{q}} \sum_{\nu\nu'} \varphi(\mathbf{p} - \mathbf{q}) n_{\mathbf{p}\nu} n_{\mathbf{q}\nu'} . \quad (74)$$

Here z is the coordination number for the nn sphere. Using the mean-field definition of the parameter $\Delta = \langle \Delta_{\mathbf{ij}} \rangle$ and the spinon energy $\varepsilon_{\mathbf{p}}$,

$$\Delta \varphi_{\mathbf{p}} = \sum_{\mathbf{q}} \varphi_{\mathbf{p}-\mathbf{q}} \tanh \frac{\varepsilon_{\mathbf{q}}}{2T} , \quad \varepsilon_{\mathbf{p}} = I \Delta \varepsilon_{\mathbf{p}} , \quad (75)$$

and the property of $\sum_{\mathbf{q}} \varphi_{\mathbf{q}} = 0$, equation (74) is reduced to

$$\mathcal{E} = I \sum_{\mathbf{p}} \varepsilon_{\mathbf{p}} n_{\mathbf{p}} . \quad (76)$$

This means that our problem is thermodynamically equivalent to the problem of spinless fermions, so the limiting value of the entropy for this system has the correct value of $S_{\infty} = N \log 2$. On the other hand, the naive mean-field treatment of the Hamiltonian (73) results in the effective Hamiltonian

$$H_{MF} = I \sum_{\mathbf{p}} \varepsilon_{\mathbf{p}\nu} n_{\mathbf{p}\nu} - \frac{I}{2} N z |\Delta|^2 \quad (77)$$

which gives a wrong value of $S_{\infty} = N \log 4$.

The nature of this discrepancy is well known. In the spin fermion representation for the spin 1/2, $\mathbf{S}_i = f_{i\nu}^\dagger \hat{\sigma} f_{i\nu}$ (where $\hat{\sigma}$ is the Pauli matrix) the local constraint $\sum_\nu f_{i\nu}^\dagger f_{i\nu} = 1$ forbids simultaneous creation of both up and down spin fermions. Since this local constraint is changed for the global constraint $N^{-1} \sum_{\mathbf{k}\nu} f_{\mathbf{k}\nu}^\dagger f_{\mathbf{k}\nu} = 1$, one should find a procedure which prevents simultaneous creation of "particle" and "hole" in the spinon spectrum when calculating the thermodynamic functions to reproduce the correct temperature behavior of entropy.

More complicated is the situation with the next model example of the Bravais lattice with two CF Kramers doublets $|G\nu\rangle, |E\nu\rangle$ and two intersite exchange coupling constants I^{GG} and I^{GE} . The system of equations (69) now describes two parameters, $\Delta^{GG}(\mathbf{u})$ given by eq. (16) and

$$\Delta^{GE}(\mathbf{u}) = I^{GE} \frac{2}{Nz} \sum_{\mathbf{k}\nu} \varphi_{\mathbf{k}} n_{\mathbf{k}\nu} |\Theta_\nu^G(\mathbf{k})|^2 = q \Delta^{GG}$$

(see eq. 72). Then the matrix Z (21) has the form

$$\frac{1}{2} \begin{pmatrix} \Delta^{GG} \varphi_{\mathbf{k}} & q \Delta^{GG} \varphi_{\mathbf{k}} & 0 & 0 \\ q \Delta^{GG} \varphi_{\mathbf{k}} & 1 & 0 & 0 \\ 0 & 0 & \Delta^{GG} \varphi_{\mathbf{k}} & q \Delta^{GG} \varphi_{\mathbf{k}} \\ 0 & 0 & q \Delta^{GG} \varphi_{\mathbf{k}} & 1 \end{pmatrix} \quad (78)$$

with normalization condition (15).

This case can be treated in the same way as the previous one, provided the intermixing of ground and excited states is not too strong, i.e., when

$$\frac{q^2}{|1 - \frac{1}{2} \Delta^{GG} \varphi_{\mathbf{k}}|} \ll 1. \quad (79)$$

Then the contribution \mathcal{E}_ζ of the half-filled lowest spin-fermion band to the energy \mathcal{E} is

$$\mathcal{E}_\zeta = \frac{\Delta_{CF}^{(0)}}{2} N^{-1} \sum_{\mathbf{k}} \sum_{\nu=\pm} n_{\mathbf{k}\nu}^\zeta \varepsilon_{\mathbf{k}\nu}^\zeta \quad (80)$$

where

$$\varepsilon_{\mathbf{k}\zeta} = \frac{1}{2} \Delta^{GG} \varphi_{\mathbf{k}} \left(1 - \frac{q^2}{|1 - \frac{1}{2} \Delta^{GG} \varphi_{\mathbf{k}}|} \right). \quad (81)$$

In this case we also have the compensation of Kramers degeneracy. It should be emphasized, however, that the second branch of the excitations generated by the matrix Z (78) is, in fact, the usual magnetic CF exciton band modified by the interaction with the spin liquid branch, and its contribution to the entropy can be treated in conventional manner, at least at $k_B T \ll \Delta_{CF}^{(0)}$.

These two examples demonstrate that there is no universal recipe for calculating the entropy in the systems with strong interplay between the non-local spin-liquid excitations and the one-site CF excitations. The third instructive example demonstrates the importance of accurate treatment of all degeneracies which could be lifted by the spin-liquid correlations. Here we consider the two-sublattice crystal with the crystal field resulting in two equivalent Kramers doublets for Ce ion in each sublattice. Then the exchange interactions in H_c and H_{nc} terms of the Hamiltonian (4) are described by four parameters $I_{\xi\xi'}^G$ and $I_{\xi\xi'}^{GE}$, where $\xi\xi' = 1, 2$. Then the matrix Z acquires the form

$$\frac{1}{2} \begin{pmatrix} \Delta_{11}^{GG} \varphi_{\mathbf{k}} & \Delta_{12}^{GG} \varphi'_{\mathbf{k}} & q \Delta_{11}^{GG} \varphi_{\mathbf{k}} & q' \Delta_{12}^{GG} \varphi'_{\mathbf{k}} \\ \Delta_{12}^{GG} \varphi'_{\mathbf{k}} & \Delta_{11}^{GG} \varphi_{\mathbf{k}} & q' \Delta_{12}^{GG} \varphi'_{\mathbf{k}} & q \Delta_{11}^{GG} \varphi_{\mathbf{k}} \\ q \Delta_{11}^{GG} \varphi_{\mathbf{k}} & q' \Delta_{12}^{GG} \varphi'_{\mathbf{k}} & 2 & 0 \\ q' \Delta_{12}^{GG} \varphi'_{\mathbf{k}} & q \Delta_{11}^{GG} \varphi_{\mathbf{k}} & 0 & 2 \end{pmatrix}$$

(this matrix represents one of two Kramers subspaces in the block-diagonal matrix $Z = Z^+ \otimes Z^-$). We assume that the in-sublattice structure factor $\varphi_{\mathbf{k}}$ and the in-sublattice coupling constants I_{11} are the same for both sublattices. Here relation between non-diagonal and diagonal elements of in-sublattice and inter-sublattice coupling constants are given by $q = I_{11}^{GE}/I_{11}^G$ and $q' = I_{12}^{GE}/I_{12}^G$, respectively. In general case the inter-sublattice structure factor $\varphi'_{\mathbf{k}} \neq \varphi_{\mathbf{k}}$. Under these assumptions $\Delta_{11} = \Delta_{22}$ and $\Delta_{12} = \Delta_{21}$, and two independent spinon parameters are determined by the equations

$$\Delta_{11}^{GG} = \frac{2}{Nz} \sum_{\mathbf{k}\nu} \varphi_{\mathbf{k}} n_{\mathbf{k}\nu} I_{11}^G |\Theta_{\nu}^G(1, \mathbf{k})|^2,$$

$$\Delta_{12}^{GG} = \frac{2}{Nz} \sum_{\mathbf{k}\nu} \varphi'_{\mathbf{k}} n_{\mathbf{k}\nu} I_{12}^G \Theta_{\nu}^G(2, \mathbf{k}) [\Theta_{\nu}^G(1, \mathbf{k})]^*. \quad (82)$$

In the case of strong intermixing ($I_{\xi\xi'} \approx 1$ and $q, q' \approx 1$) all the coefficients $|\Theta_{\nu}^G(\xi, \mathbf{k})|$ are of the same order, and each of them can be estimated as $\theta \approx 1/2\sqrt{2}$. As a result, the contribution of the lowest branches $\varepsilon_{\mathbf{k}\nu}^{\zeta}$ at low temperatures $k_B T \ll \Delta_{CF}^{(0)}$ can be approximately represented as

$$\mathcal{E}_{\zeta} \approx \frac{1}{8} \Delta_{CF}^{(0)} N^{-1} \sum_{\mathbf{k}} \sum_{\nu=\pm} n_{\mathbf{k}\nu}^{\zeta} \varepsilon_{\mathbf{k}\nu}^{\zeta} \quad (83)$$

because in this case all terms in the matrix \mathbf{Z} related to lowest branches ζ contain the factors Δ^G , as was explicitly demonstrated in the above example (see eq. 81).

Again we see that the diagonalization procedure (17) results in a non-universal form of the average energy for spin liquid excitations in comparison with corresponding equations for the conventional Fermi liquids, at least at low temperatures.

Parameters	High quality	S.Nolten et.al.
\mathcal{T}_1	16.15 K	14.40 K
\mathcal{T}_2	24.65 K	12.40 K
\mathcal{G}_1	1.83 K	3.00 K
\mathcal{G}_2	-6.60 K	-5.41 K
$\tilde{\Delta}_{CF}$	-2.0 K	8.0 K
a	0.53	0.62

Table 1. Parameters which define the spinon spectrum in the samples of higher and lower quality

Figure captions

Fig.1 Magnetostriction λ of single-crystalline CeNiSn for a field directed along the a -axis (bold lines) and elongation (or contraction) along the a , b and c -axis (thin solid, dotted and dashed lines, respectively) at temperatures of 0.5 K (a), 1.4 K (b), and 4.3 K (c).

Fig.2 Coefficient of magnetostriction λ' of single-crystalline CeNiSn for a field directed along the a -axis. All notations are the same as in fig. 1

Fig.3: Field and temperature dependence of the logarithmic volume derivative of magnetic susceptibility evaluated from eq. (3) (the isothermal compressibility is $\kappa_T = 1.8 * 10^{-11} \text{ m}^2/\text{N}$ according to [21]): (a) field dependence for $T = 0.5 \text{ K}$ (squares), $T = 1.4 \text{ K}$ (diamonds) and $T = 4.3 \text{ K}$ (triangles); (b) temperature dependence for different magnetic fields.

Fig.4: Orthorhombic CeNiSn lattice, structure of bc -plane. Two Ce sublattices are denoted by black and grey circles, respectively. The orthorhombic distortion \mathcal{O} (solid arrows) transforms the simple hexagonal lattice into two-sublattice orthorhombic one. The in-sublattice interaction \mathcal{T}_1 is denoted by solid double arrow. The inter-sublattice interaction \mathcal{T}_2 and \mathcal{G}_2 is denoted by dashed double arrow.

Fig.5: Fragments of the density of states (DOS) of spinon spectra for high quality sample (bold line) and imperfect sample (thin line).

Fig.6: Temperature dependence of heat capacity. Dashed line represents the spin-fermion contribution γ_{sp} , for imperfect sample, and solid line gives the Sommerfeld coefficient with additional contribution from conduction electrons $\gamma_{cond} = 8 \text{ mJ/mol K}^2$. The spinon part calculated for high quality sample is presented in the insert. Experimental points for perfect sample are taken from [5] (triangles) and those for imperfect sample are taken from [17] (squares).

Fig.7: Scattering functions of inelastic magnetic neutron scattering in absolute units calculated for high quality (bold line) and less perfect sample (thin line).

Fig.8: Calculated magnetic susceptibility (line) compared with experimental data for specimen # 4 from Ref. [5].

Fig.9: Calculated linear coefficient of volume expansion (line) compared with experimental data [17] (triangles). Inset: temperature dependence of logarithmic derivatives of entropy.

Fig.10: Calculated coefficients of linear expansion (lines) compared with experimental data [13] (points) along a- (solid line, squares), b- (dashed line, triangles) and c-axis (dotted line, diamonds).

Fig.11: Components of volume derivative of magnetic susceptibility calculated from eq. (62)

Fig.12: Logarithmic derivative of magnetic susceptibility calculated from eq. (62) (solid line) and extracted from experiment [21] (circles).

-
- [1] Takabatake T., Fujii H.: Jpn. J. Appl. Phys. Ser. 8, 254 (1993).
- [2] T. Takabatake, T. Yoshino, H. Tanaka, Y. Bando, H. Fujii, T. Fujita, H. Shida, and T. Suzuki. Physica B **206&207**, 804 (1995).
- [3] G. Aeppli and Z. Fisk, Comments Cond. Mat. Phys., **16**, 155 (1992).
- [4] T. Takabatake, F. Iga, T. Yoshino, Y. Echizen, K. Katoh, K. Kobayashi, M. Higa, N. Shimizu, Y. Bando, G. Nakamoto, H. Fujii, K. Izawa, T. Suzuki, T. Fujita, M. Sera, M. Hiroi, K. Maezawa, S. Mock, H. v. Löhneysen, A. Brückl, K. Neumaier, and K. Andres, J. Magn. Magn. Mat. **177-181**, 277 (1998).
- [5] T. Takabatake, G. Nakamoto, T. Yoshino, H. Fujii, K. Izawa, S. Nishigori, H. Goshima, T. Suzuki, T. Fujita, K. Maezawa, T. Hiraoka, Y. Okayama, I. Oguro, A.A. Menovsky, K. Neumaier, A. Brückl, and K. Andres, Physica B **223&224**, 413 (1996).
- [6] K. Nakamura, Y. Kitaoka, K. Asayama, T. Takabatake, G. Nakamoto, H. Tanaka, and H. Fujii, Physica B **206&207**, 829 (1995).
- [7] T.E. Mason, G. Aeppli, A.P. Ramirez, K.N. Clausen, C. Broholm, N. Stücheli, E. Bucher, and T.T.M. Palstra, Phys. Rev. Lett. **69** 490 (1992).
- [8] T. Sato, H. Kadowaki, H. Yoshizawa, T. Ekino, T. Takabatake, H. Fujii, L.P. Regnault, and Y. Ishikawa, J. Phys.: Cond. Mat. **7**, 8009 (1995).
- [9] H. Ikeda and K. Miyake, J. Phys. Soc. Jpn. **65**, 1769 (1996).
- [10] P.S. Riseborough, Phys. Rev. B **45**, 13984 (1992).
- [11] Y. Ono, T. Matsuura, and Y. Kuroda, Journ. Phys. Soc. Jpn., **63**, 1406 (1994).
- [12] Yu. Kagan, K.A. Kikoin K.A, and N.V. Prokof'ev, JETP. Lett. **57**, 600 (1993).
- [13] K.A. Kikoin, A. de Visser, K. Bakker and T. Takabatake, Z.Phys. B **94**, 79 (1994).
- [14] P.A. Alekseev, V.N. Lazukov, E.S. Clementyev, E.V. Nefedova, I.P. Sadikov, M. N. Chlopkov, A.Yu. Muzicka, I.L. Sashin, N.N. Efremova and V. Bührer, JETP, **79**, 665 (1994).
- [15] Yu. Kagan, K.A. Kikoin and A.S. Mishchenko, Phys. Rev. B **55**, 12348 (1997).
- [16] K.A. Kikoin, M.N. Kiselev and A.S. Mishchenko, JETP Letters **60**, 600 (1994); Physica B **206&207**, 129 (1995).
- [17] A.J. Nolten, A. de Visser, F.E. Kayzel, J.J.M. Franse, H. Tanaka, and T. Takabatake, Physica B **206-207**, 825 (1995).
- [18] K.A. Kikoin, M.N. Kiselev and A.S. Mishchenko, Czech. J. Phys. **46**, 1899 (1996).
- [19] S. Holtmeier, P. Haen and Y. Ishikawa, Physica B **223&224**, 429 (1996); S. Holtmeier, Ph.D. Thesis, University Joseph Fourier (Grenoble, 1994).
- [20] B.S. Chandrasekhar and F. Fawcett, Adv. Phys. **20**, 775 (1971).
- [21] Uwatoko (1994), unpublished.
- [22] B. Cornut and B. Coqblin, Phys. Rev. B, **5**, 4541 (1972).
- [23] B.R. Cooper, R. Siemann, D. Yang, P. Thayamballi, and A. Banerjee, in *The Handbook on the Physics and Chemistry of Actinides*, edited by A.J. Freeman and G.H. Lander (North-Holland, Amsterdam, 1985), Vol. 2, Chap. 6, pp. 435-500.
- [24] P.W. Anderson, Mater. Res. Bull., **8**, 153 (1973).
- [25] P. Coleman and N. Andrei, J. Phys.: Cond. Mat. **1**, 4057 (1989).
- [26] K.A. Kikoin, M.N. Kiselev and A.S. Mishchenko, Physica B **230-232**, 490 (1997).
- [27] A. A. Abrikosov, Physics **2**, 21 (1965).
- [28] T. Takabatake, F. Teshima, H. Fujii, S. Nishigori, T. Suzuki, T. Fujita, Y. Yamaguchi, J. Sakurai and D. Jaccard, Phys. Rev. B **41** 9607 (1990).
- [29] I. Higashi, K. Kobayashi, T. Takabatake, and M. Kasaya, J. Alloys and Compounds **193**, 300 (1993).
- [30] J.-G. Park, D.T. Adroja, K.A. McEwen, Y.J. Bi, and J. Kulda, *Proc. Int. Conf. SCES98*, Paris, 1998, to be published in Physica B.
- [31] T. Tanamoto, K. Kuboki and H. Fukuyama, J. Phys. Soc. Jap. **60**, 4395 (1991).
- [32] D.R. Grempel and M. Lavagna, Solid State Comm. **83**, 595 (1992).
- [33] G. Nakamoto, T. Takabatake, Y. Bando, H. Fujii, K. Izawa, T. Suzuki, T. Fujita, A. Minami, I. Oguro, L.T. Tai, and A.A. Menovski **206&207**, 840 (1995).
- [34] S. Kambe, S. Raymond, H. Suderow, J. McDonough, B. Fak, L.P. Regnault, and Y. Ishikawa, Physica B **223&224**, 135 (1996).
- [35] D.C. Mattis, *The Theory of Magnetism* (Harper & Row, N.Y., 1965).
- [36] A.S. Mishchenko, JETP Letters, **66**, 487 (1997).
- [37] J.H.O. Varley, Proc. Roy. Soc. **A267**, 413 (1956).
- [38] E.R. Callen and H.B. Callen, Phys. Rev. **129**, 578 (1963).
- [39] C.L. Kane, P. Lee, and N. Read, Phys. Rev. **B39**, 6880 (1989).
- [40] G. Khaliullin and P. Horsch, Phys. Rev. **B47**, 463 (1993).

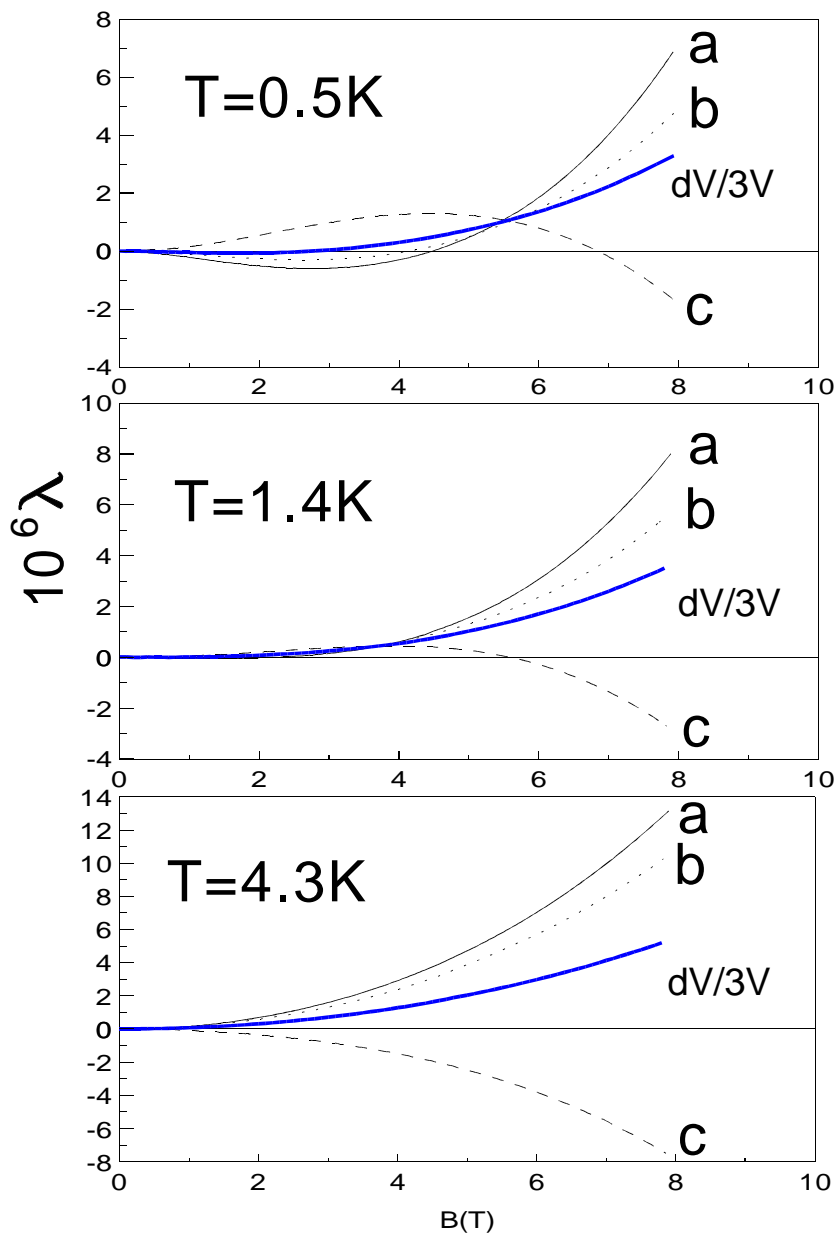


Fig. 1.

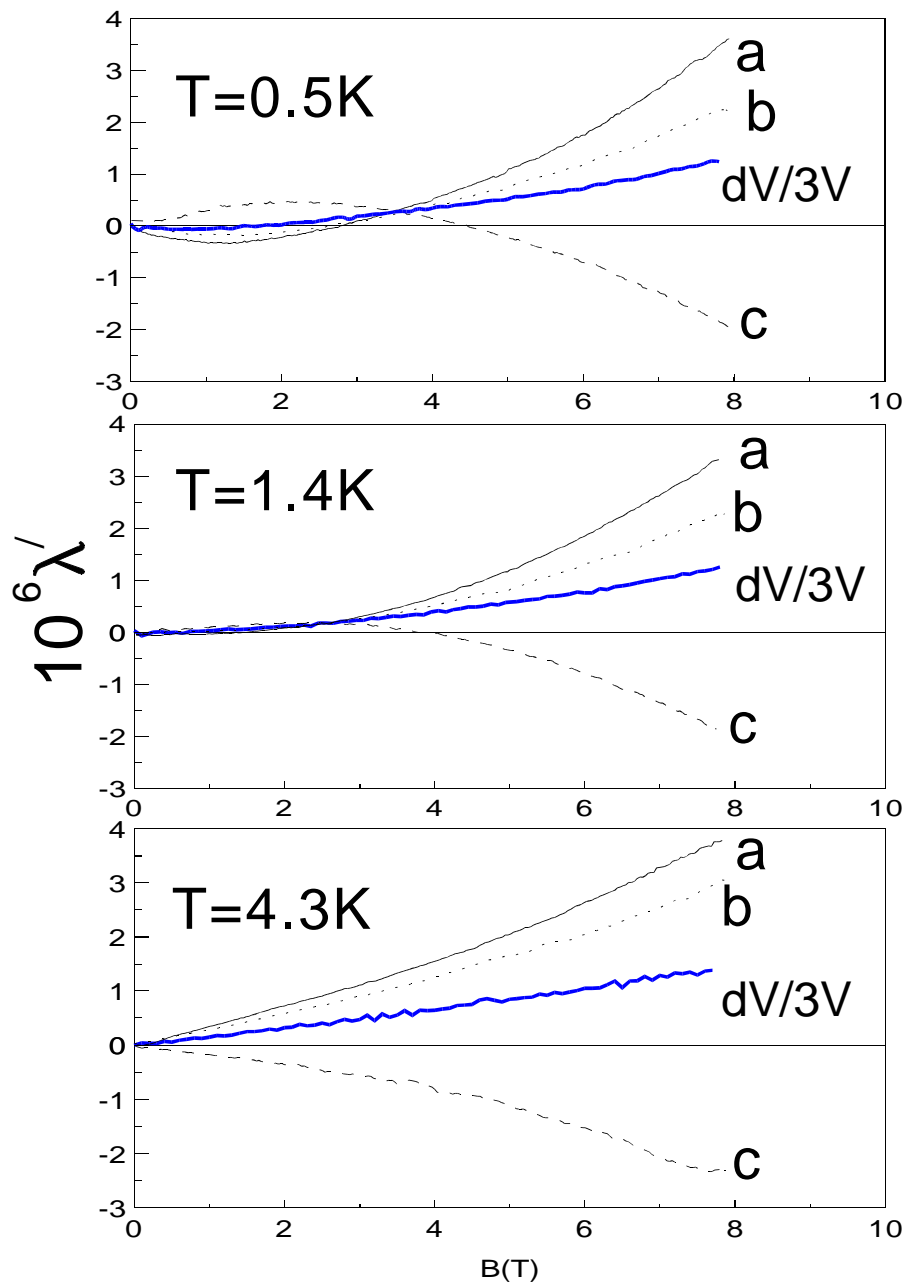


Fig. 2.

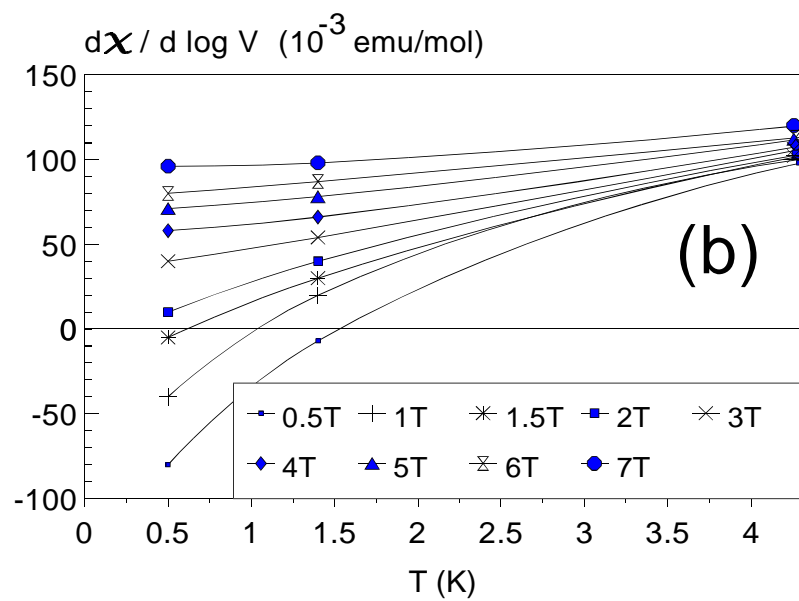
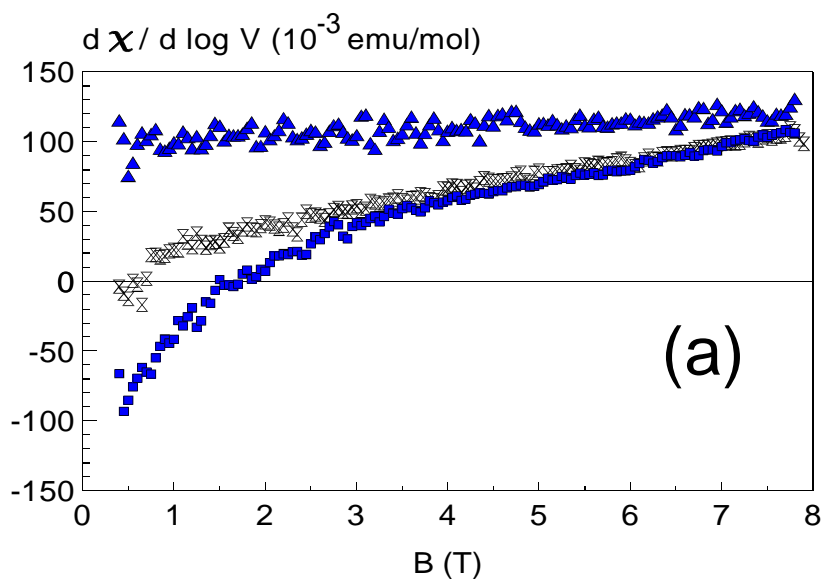


Fig. 3.

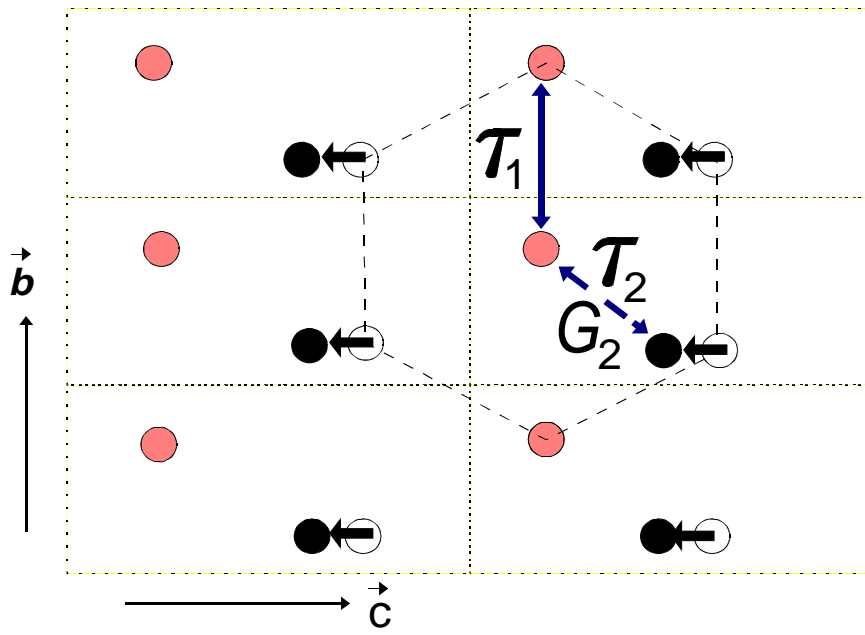


Fig. 4.

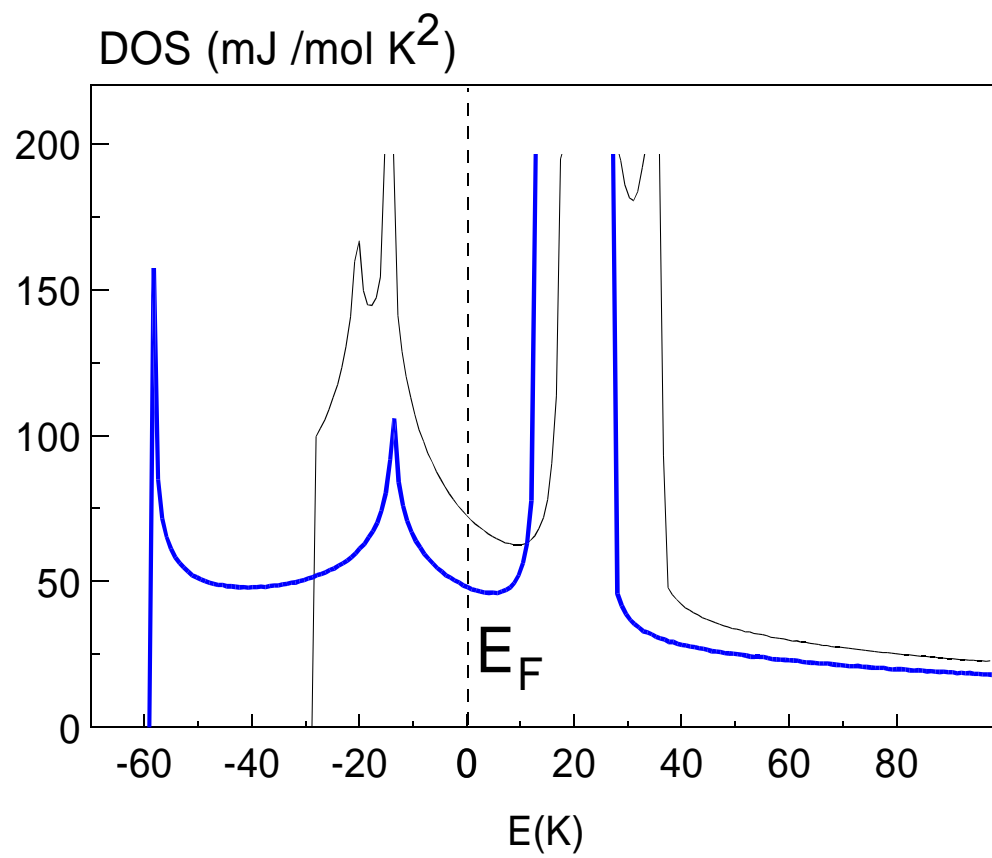


Fig. 5.

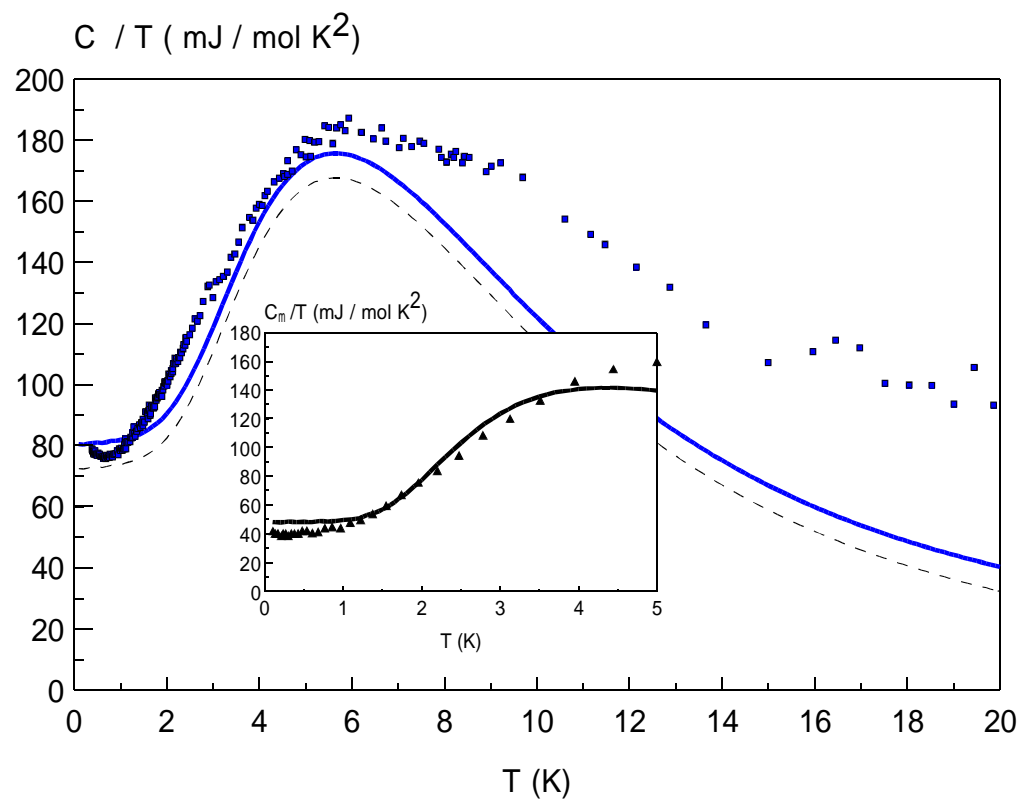


Fig. 6.

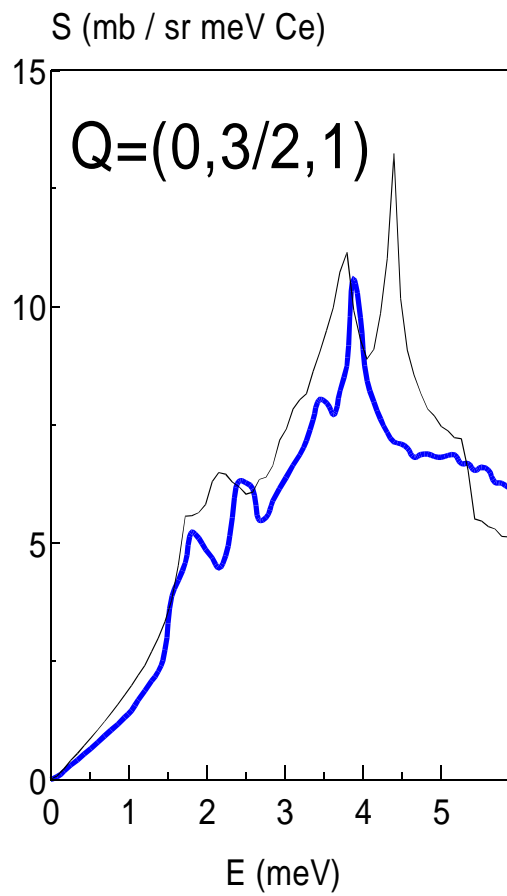
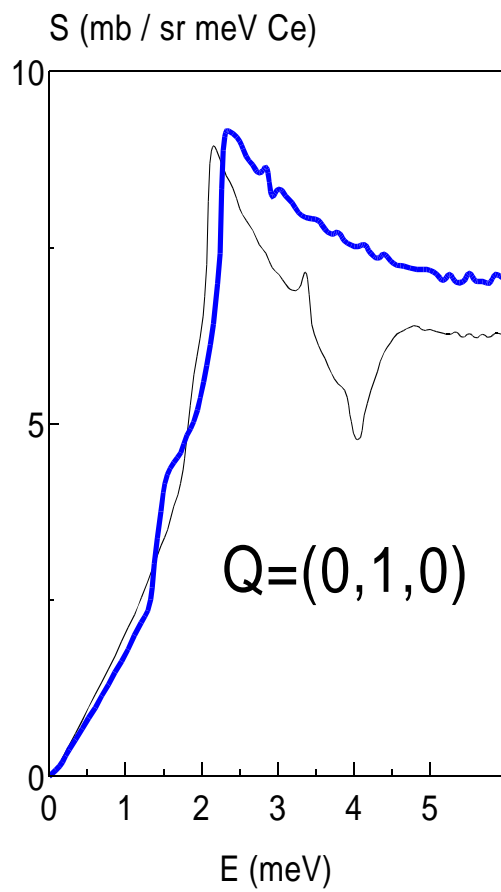


Fig. 7.

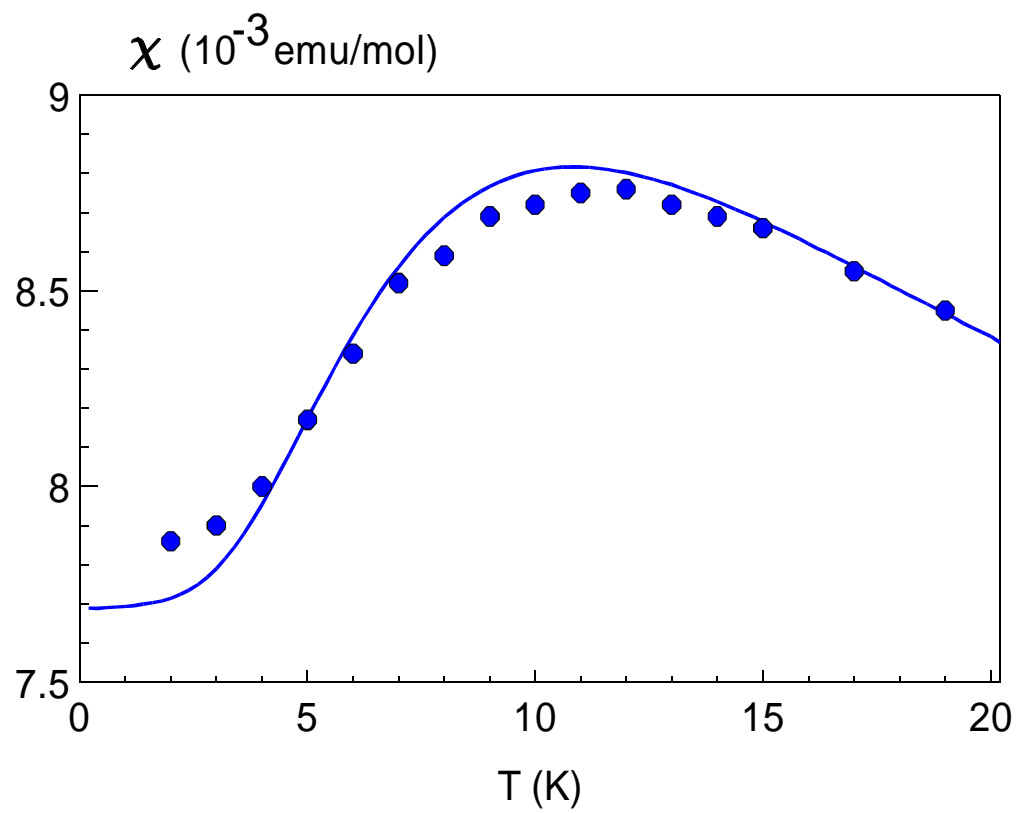


Fig. 8.

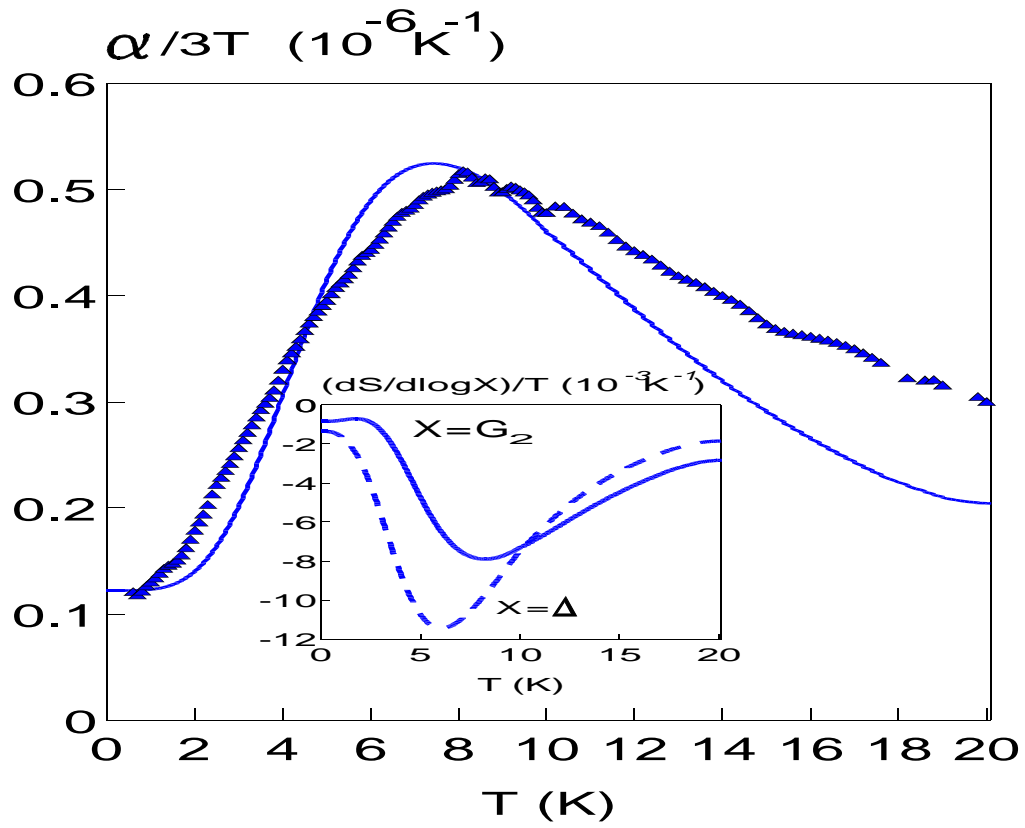


Fig. 9.

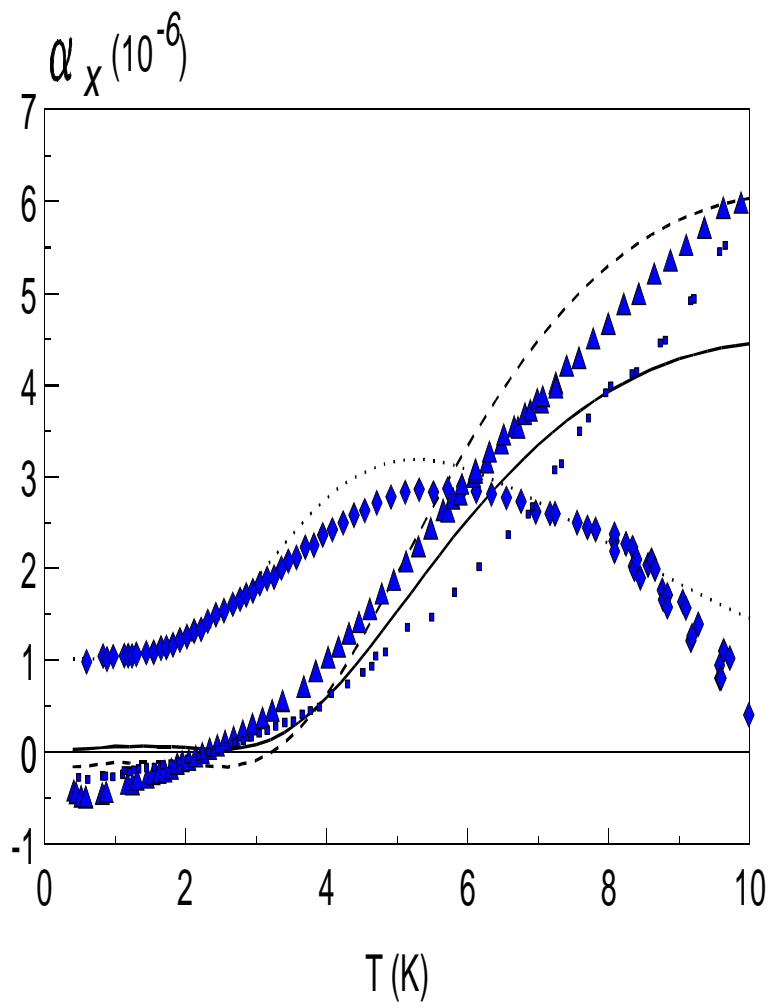


Fig. 10.

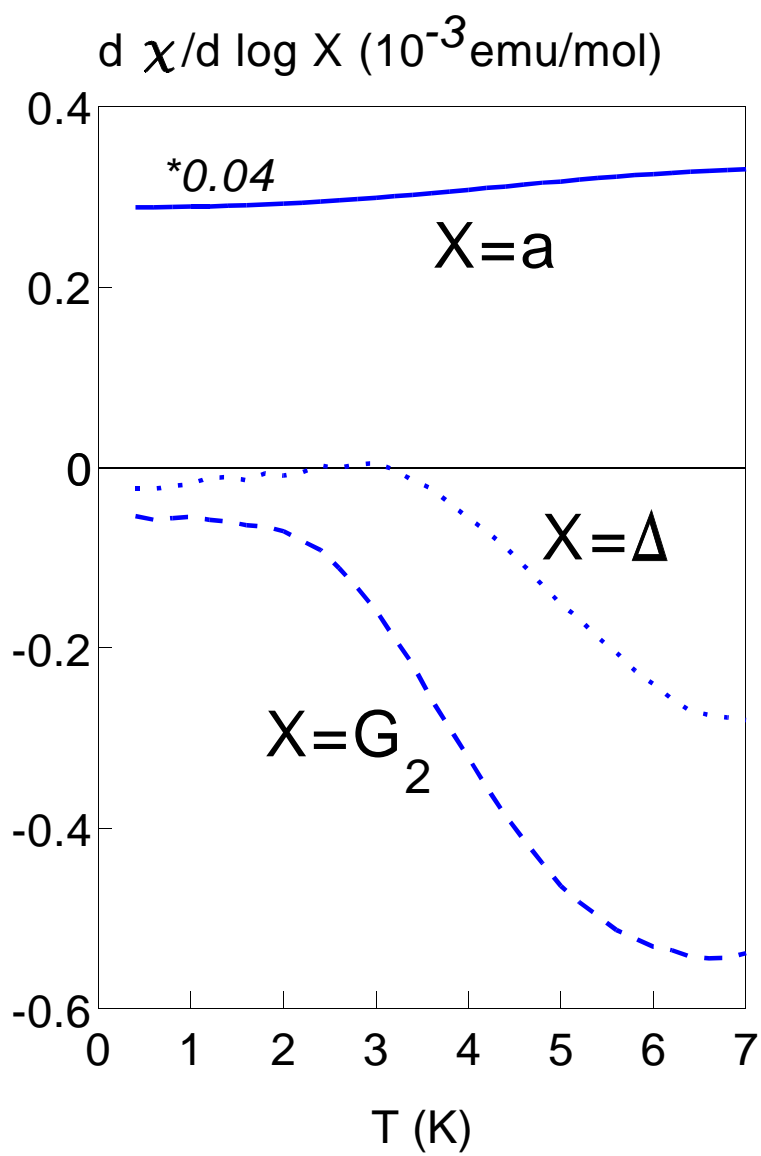


Fig. 11.

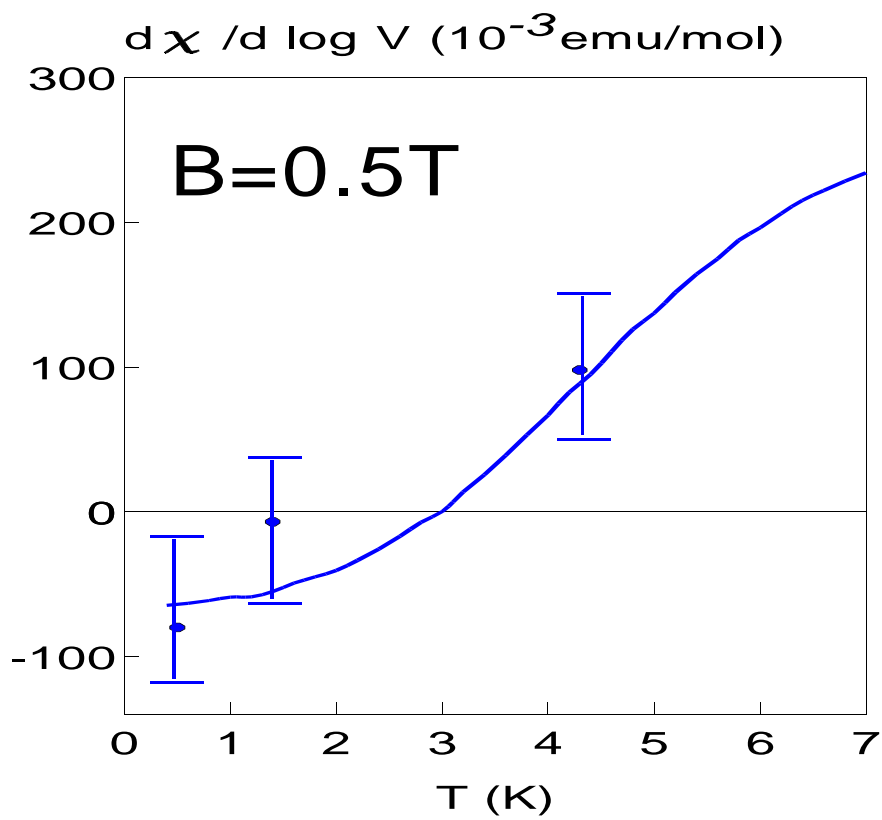


Fig. 12.